Meteoritics & Planetary Science 36, 975–997 (2001)
Available online at http://www.uark.edu/meteor

Aluminum-26 in calcium-aluminum-rich inclusions and chondrules from unequilibrated ordinary chondrites

GARY R. HUSS[1,3]*, GLENN J. MACPHERSON[2], G. J. WASSERBURG[1], SARA S. RUSSELL[2,4] AND GOPALAN SRINIVASAN[1,5]

[1]Division of Geological and Planetary Sciences, Mail Code 170-25, California Institute of Technology, Pasadena, California 91125, USA
[2]Department of Mineral Sciences, National Museum of Natural History, Smithsonian Institution, Washington, D.C. 20560-0119, USA
[3]Department of Geological Sciences and Center for Meteorite Studies, Arizona State University, P.O. Box 871404, Tempe, Arizona 85287-1404, USA
[4]Department of Mineralogy, The Natural History Museum, Cromwell Road, London SW7 5BD, U.K.
[5]Physical Research Laboratory, Navrangpura, Ahmedabad 380-009, India
*Correspondence author's e-mail address: gary.huss@asu.edu

(Received 2000 June 12; accepted in revised form 2001 April 26)

Abstract–In order to investigate the distribution of ^{26}Al in chondrites, we measured aluminum-magnesium systematics in four calcium-aluminum-rich inclusions (CAIs) and eleven aluminum-rich chondrules from unequilibrated ordinary chondrites (UOCs). All four CAIs were found to contain radiogenic ^{26}Mg ($^{26}Mg^*$) from the decay of ^{26}Al. The inferred initial $^{26}Al/^{27}Al$ ratios for these objects ($(^{26}Al/^{27}Al)_0 \approx 5 \times 10^{-5}$) are indistinguishable from the $(^{26}Al/^{27}Al)_0$ ratios found in most CAIs from carbonaceous chondrites. These observations, together with the similarities in mineralogy and oxygen isotopic compositions of the two sets of CAIs, imply that CAIs in UOCs and carbonaceous chondrites formed by similar processes from similar (or the same) isotopic reservoirs, or perhaps in a single location in the solar system. We also found $^{26}Mg^*$ in two of eleven aluminum-rich chondrules. The $(^{26}Al/^{27}Al)_0$ ratio inferred for both of these chondrules is $\sim 1 \times 10^{-5}$, clearly distinct from most CAIs but consistent with the values found in chondrules from type 3.0–3.1 UOCs and for aluminum-rich chondrules from lightly metamorphosed carbonaceous chondrites ($\sim 0.5 \times 10^{-5}$ to $\sim 2 \times 10^{-5}$). The consistency of the $(^{26}Al/^{27}Al)_0$ ratios for CAIs and chondrules in primitive chondrites, independent of meteorite class, implies broad-scale nebular homogeneity with respect to ^{26}Al and indicates that the differences in initial ratios can be interpreted in terms of formation time. A timeline based on ^{26}Al indicates that chondrules began to form 1 to 2 Ma after most CAIs formed, that accretion of meteorite parent bodies was essentially complete by 4 Ma after CAIs, and that metamorphism was essentially over in type 4 chondrite parent bodies by 5 to 6 Ma after CAIs formed. Type 6 chondrites apparently did not cool until more than 7 Ma after CAIs formed. This timeline is consistent with ^{26}Al as a principal heat source for melting and metamorphism.

INTRODUCTION

Chondrules and calcium-aluminum-rich inclusions (CAIs) are two important primary constituents of chondritic meteorites. Both formed at high temperatures early in solar system history and record the timing and conditions in the earliest stages of solar system formation. Yet neither the genetic relationship between these two groups of objects nor their relative formation ages are well understood. The expected duration of the active phase of the solar nebula is on the order of a few $\times 10^6$ years, but time differences of significantly less than 10^6 years at 4.56 Ga cannot currently be measured using long-lived radiochronometers. Short-lived radionuclides that were present in the early solar system but are now extinct provide one way to resolve such small time differences.

The most widely studied short-lived radionuclide is ^{26}Al (half-life, $t_{1/2}$ = 730 000 years), which decays to radiogenic ^{26}Mg ($\equiv {}^{26}Mg^*$). Its presence in the early solar system is well established (*e.g.*, Lee *et al.*, 1976, 1977; review by MacPherson *et al.*, 1995). While giving no information about absolute ages, differences in inferred initial $^{26}Al/^{27}Al$ ratios ($(^{26}Al/^{27}Al)_0$) potentially can discriminate between events separated by as little as $\sim 10^5$ years (Lee *et al.*, 1976; Hsu *et al.*, 2000). Unfortunately, the usefulness of ^{26}Al as a chronometer for studying the relative formation times of CAIs and chondrules is clouded by the possibility that it was not uniformly distributed

Prelude preprint MS#4390

throughout the early solar system (*e.g.*, Wood, 1996a). Most CAIs consistently show evidence for high initial ratios, $(^{26}Al/^{27}Al)_0 \approx 5 \times 10^{-5}$. No incontrovertible evidence of higher values is found in CAIs. However, rare CAI types such as the FUN inclusions (named for extreme isotopic Fractionated and Unidentified Nuclear isotopic anomalies; Wasserburg *et al.*, 1977) and hibonite-fassaite microspherules (*e.g.*, Ireland *et al.*, 1991; Russell *et al.*, 1998) have considerably lower $(^{26}Al/^{27}Al)_0$ values and, at the same time, retain large endemic nuclear isotopic anomalies inherited from their precursor presolar dust. Thus, their low $(^{26}Al/^{27}Al)_0$ values are not easily attributable to later formation or reprocessing (*e.g.*, Wasserburg and Papanastassiou, 1982; MacPherson *et al.*, 1995). The solar system was isotopically heterogeneous at some scale; certainly presolar dust grains were the original solid materials in the solar nebula. Some workers argue that large regions of the solar nebular differed from one another isotopically (Lee *et al.*, 1979; Wood, 1996a), while others conclude that heterogeneity was minor on a macroscopic scale (MacPherson *et al.*, 1995). To explain the range in $(^{26}Al/^{27}Al)_0$ by heterogeneity requires a least an order of magnitude variation in this ratio in substantial regions of the nebula. This should be associated with other isotopic effects.

One approach to the problem of initial ^{26}Al uniformity is to analyze CAIs and chondrules from a variety of chondrite types, on the assumption that the different chondrite classes sampled different nebular regions and hence provide some estimate of the degree of isotopic homogeneity in the solar system. Therefore, we carried out a search for and analysis of the chemical and isotopic properties of CAIs and chondrules in unequilibrated ordinary chondrites (UOCs). Here we faced two experimental difficulties. First, the rarity of CAIs in ordinary (and enstatite) chondrites makes such investigations difficult. Second, aluminum-rich phases are rare in chondrules. With $(^{26}Al/^{27}Al)_0 = 5 \times 10^{-5}$ and Al/Mg of ~0.1 in material of chondritic composition, the enrichment in $^{26}Mg/^{24}Mg$ would be only ~50 ppm. For ion probe measurements, which have uncertainties of 1–2‰, Al/Mg ratios of >10 are required to detect $^{26}Mg^*$ from $(^{26}Al/^{27}Al)_0 = 5 \times 10^{-5}$, and higher Al/Mg ratios are required for lower initial abundances. Suitable ratios are found in aluminum-rich phases such as plagioclase and, occasionally, glass, but are not found in the most common chondrule minerals such as olivine and pyroxene. We overcame these problems by using systematic x-ray area mapping of large numbers of polished UOC thin sections to find CAIs and relatively rare aluminum-rich chondrules that contain plagioclase and aluminum-rich glass.

Prior to our study, ~10 plagioclase-bearing UOC chondrules had been analyzed isotopically (Hutcheon *et al.*, 1989, 1994; Kennedy *et al.*, 1992; Hutcheon and Jones, 1995) and no evidence for ^{26}Al was found in any of them. Only a few meteoritic constituents other than CAIs from carbonaceous chondrites had been found to contain $^{26}Mg^*$. The positive cases included 2 of 12 plagioclase-olivine inclusions (POIs) from Allende (CV3) examined by Sheng *et al.* (1991), which exhibited $(^{26}Al/^{27}Al)_0 \approx (3–6) \times 10^{-6}$; a hibonite-spinel CAI fragment from Dhajala (H3.8) with $(^{26}Al/^{27}Al)_0 \approx 8 \times 10^{-6}$ (*e.g.*, Hinton and Bischoff, 1984); an olivine-pyroxene-anorthite clast from Semarkona (LL3.0) with $(^{26}Al/^{27}Al)_0 \approx 8 \times 10^{-6}$ (Hutcheon and Hutchison, 1989); a glass inclusion from Bovedy (L3.7) with $(^{26}Al/^{27}Al)_0 \approx 3 \times 10^{-7}$ (Hutcheon *et al.*, 1989); and plagioclase crystals of unknown petrologic context, separated from a bulk sample of St. Marguerite (H4), that showed $(^{26}Al/^{27}Al)_0 \approx 2 \times 10^{-7}$ (Zinner and Göpel, 1992).

In this paper, we present complete aluminum-magnesium data for four CAIs and eleven aluminum-rich chondrules, including data for two CAIs and nine chondrules that have not been published previously except in summary form. Initial isotopic results for some of the objects in our study have been reported previously (Srinivasan *et al.*, 1996; Russell *et al.*, 1996a, 1997). Since our study was initiated, other workers have found a number of chondrules containing ^{26}Al (Srinivasan *et al.*, 2000a,b; Kita *et al.*, 2000; Hutcheon *et al.*, 2000; McKeegan *et al.*, 2000; Marhas *et al.*, 2000; Mostefaoui *et al.*, 1999, 2000). In this paper, we summarize all of our new data and data available in the literature and discuss the current situation with regard to ^{26}Al in the early solar system. This work is part of a broader study to investigate the relationships between CAIs, aluminum-rich chondrules, and "ordinary" ferromagnesian chondrules. The compositional relationships have been treated briefly by MacPherson and Huss (2000), and a more complete treatment is in preparation. Related studies of oxygen isotopes in two of the CAIs and in several of the aluminum-rich chondrules are described in McKeegan *et al.* (1998) and Russell *et al.* (2000).

METHODS

Identification and Characterization of Aluminum-Rich Chondrules and Calcium-Aluminum-Rich Inclusions

Polished thin sections of unequilibrated H, L, and LL chondrites from the Smithsonian collection were examined by optical microscope and then studied using the Smithsonian JEOL JSM-840A scanning electron microscope, equipped with a Kevex Si(Li) x-ray analyzer. CAIs and aluminum-rich chondrules were located by systematically searching each thin section by x-ray area mapping, at a spatial resolution sufficient to detect any aluminum-rich objects greater than ~10 μm in size.

Aluminum-Magnesium Measurements

Magnesium isotopes were measured with PANURGE, a modified CAMECA IMS-3f ion microprobe, using standard techniques (Huneke *et al.*, 1983; Fahey *et al.*, 1987). A mass resolving power of ~2800, sufficient to resolve $^{24}MgH^+$ from $^{25}Mg^+$ and $48Ca^{++}$ from $^{24}Mg^+$, was used. Instrumental mass fractionation, which differs among minerals of interest, was

accounted for by comparing measured $^{25}Mg^{+}/^{24}Mg^{+}$ ratios for mineral standards with the $^{25}Mg/^{24}Mg$ of terrestrial Mg (0.12663; Catanzaro *et al.*, 1966) and is given in permil (= ‰) per amu by:

$$\Delta^{25}Mg = \left(\frac{\left(^{25}Mg/^{24}Mg\right)_{meas}}{0.12663} - 1 \right) \times 1000$$

Standards were Burma spinel, Madagascar hibonite, chromium diopside, San Carlos olivine, Miakajima plagioclase, and synthetic melilite glass. The intrinsic isotopic mass fractionation for sample minerals (F_{Mg}) was found by subtracting the mean $\Delta^{25}Mg$ for the appropriate standard mineral from the $\Delta^{25}Mg$ measured for the sample. Instrumental fractionation for each mineral is reproducible to ±2‰, so F_{Mg} values that exceed this uncertainty are considered significant.

After correcting for instrumental mass fractionation using a linear law (*i.e.*, assuming that the fractionation for $^{26}Mg/^{24}Mg$ is twice that for $^{25}Mg/^{24}Mg$), the $^{26}Mg/^{24}Mg$ ratio obtained for several mineral standards was 0.13955, the value typically found by PANURGE (*e.g.*, Hutcheon and Hutchison, 1989). Shifts in $^{26}Mg/^{24}Mg$ remaining for sample minerals after accounting for both instrumental and intrinsic mass fractionation are reported in permil relative to terrestrial $^{26}Mg/^{24}Mg$:

$$\delta^{26}Mg = \left(\frac{\left(^{26}Mg/^{24}Mg\right)_{corr}}{0.13955} - 1 \right) \times 1000$$

Differences in ionization efficiency between Al and Mg were accounted for by comparing the measured $^{27}Al^{+}/^{24}Mg^{+}$ to the $^{27}Al/^{24}Mg$ ratio for each standard mineral. All data are reported with 2σ uncertainties.

RESULTS

Petrography and Mineral Chemistry of the Aluminum-Rich Objects

Four CAIs and eleven aluminum-rich chondrules were studied in detail. Petrographic descriptions and summaries of the mineral chemistry for the CAIs are given below. The characteristics of the aluminum-rich chondrules are also summarized here. Detailed descriptions of the chondrules, including bulk major and trace element compositions, will appear in a separate paper (MacPherson and Huss, in preparation).

Calcium-Aluminum-Rich Inclusions–Semarkona 4128-3-1 (Fig. 1a) is a ~320 × 130 μm, irregularly shaped type A inclusion. The interior is a dense, polygonal-granular intergrowth of equant melilite crystals ($Åk_{7-15}$; ≤30 μm) that enclose tiny grains of spinel (≤5 μm) and less abundant perovskite (≤2 μm). Much of the contorted outer surface (and also cavities in the CAI interior) is rimmed by a 2–4 μm layer of aluminous diopside, suggesting that this CAI was incorporated into the parent meteorite in its present form. In the outer parts, melilite is corroded and embayed by secondary sodalite.

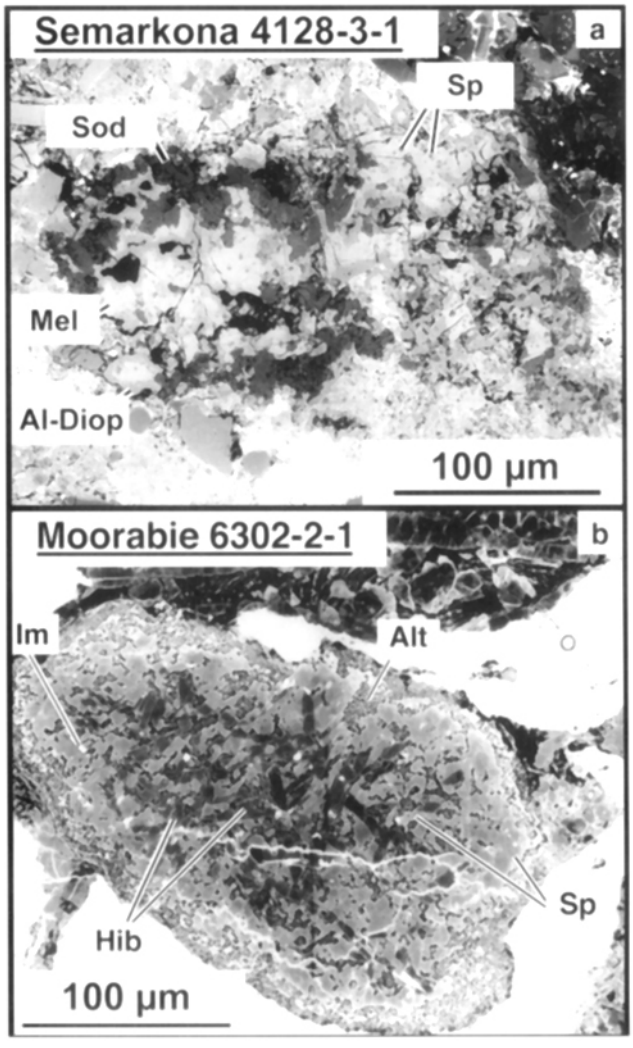

FIG. 1. (a) Backscattered electron image of an irregularly shaped type A inclusion in Semarkona. The inclusion consists of melilite (Mel), spinel (Sp), and minor perovskite (bright grains). Note the pervasive secondary sodalite (Sod) in the outer parts of the inclusion and the aluminous diopside (Al-Diop) on the rim. (b) Backscattered electron image of a compact hibonite-spinel inclusion from Moorabie. The inclusions consists of a core of densely intergrown hibonite (Hib) laths and spinel (Sp) surrounded by a spinel-rich mantle. The inclusion is heavily embayed by a fine-grained intergrowth of secondary sodalite and phyllosilicate (Alt). Original perovskite appears to have been altered to ilmenite (Im).

Semarkona 1805-2-1 is a compact lens-shaped inclusion, ~480 μm in maximum dimension, that was first described by Bischoff and Keil (1984); also see Fig. 10.3.17 of MacPherson *et al.* (1988). It consists mostly of densely intergrown, blue-pleochroic, hibonite laths (TiO_2 ~3 to7%; MgO up to 3%) ~20–40 μm across and spinel (FeO ≤0.4%), with subordinate irregular melilite ($Åk_{1-10}$) crystals and scattered grains of perovskite. One portion of the inclusion is fragmented and

porous. Remnants of a thin (~10 μm) mantle of melilite ($Åk_{\sim 18}$) are present at several locations around the periphery. These locations also contain the only vestiges of a rim sequence that consists of an inner layer of anorthite (An_{99}) and an outer layer of fassaite.

Moorabie 6302-2-1 (Fig. 1b) is a compact elliptical CAI, ~150 × 275 μm, consisting mostly of a fine-grained, dense intergrowth of hibonite blades (≤40 μm; 0.6–4 wt% MgO, 0.7–7% TiO_2, 1–6% FeO) and spinel (12–14% FeO, 1–5% Cr_2O_3). Rounded and equant ilmenite grains (~5 μm) are enclosed in both spinel and hibonite, and their shapes indicate that they formed from perovskite. The spinel + hibonite intergrowth is heavily embayed by an extremely fine-grained intergrowth of sodalite and phyllosilicate (?) that has propagated along grain boundaries; this secondary assemblage preferentially corrodes and partly replaces spinel rather than hibonite. Spinel and hibonite crystals show slight compositional zoning, with FeO and Cr_2O_3 more enriched on the outside of crystals and along fractures.

Quinyambie 6076-5-1 (Fig. 1A in Russell *et al.*, 1996a; called Moorabie in that paper because the two meteorites were then believed to be paired) is a discontinuous chain-like CAI, ~170 μm in maximum dimension. It consists of discrete clumps of melilite ($Åk_{1-5}$) that enclose subordinate spinel crystals (FeO up to 2%), blocky ~2–4 μm perovskite grains, and rare ~10 μm long hibonite laths. The individual melilite clumps are separated from one another by meteorite matrix. Each clump has a discontinuous thin (~1–2 μm) rim of aluminous diopside.

Aluminum-Rich Chondrules–The group of objects collectively referred to as aluminum-rich chondrules is diverse, and separate names for different varieties have arisen that are based mostly on individual mineralogical or chemical properties (*e.g.*, Bischoff and Keil, 1984; Sheng *et al.*, 1991). This proliferation of names obscures the probability that these objects are all related. Therefore, we adopt a different approach from those earlier workers. We term these chondrules collectively as "Al-chondrules" and adopt a nomenclature system that is grounded in phase equilibria. Specifically, we utilize a system based on chondrule bulk compositions as plotted in a petrogenetically-relevant phase diagram within the $CaO–MgO–Al_2O_3–SiO_2$ system (Fig. 2). It is clear from Fig. 2 that Al-chondrule bulk compositions (even some with significant FeO) mostly lie along a single continuous trend extending from near the mineral anorthite toward the forsterite (Mg_2SiO_4) apex, and crossing both the forsterite (+ spinel) and anorthite (+ spinel) phase volumes. Chondrules whose bulk compositions plot in the anorthite (+ spinel) phase field and which have abundant euhedral calcic plagioclase crystals are termed plagioclase-rich Al-chondrules. Two-thirds of the so-called plagioclase-olivine inclusions (POIs) studied by Sheng *et al.* (1991) are what we define as plagioclase-rich Al-chondrules. Those Al-chondrules that plot in the forsterite (+ spinel) field, and which commonly contain large euhedral olivine phenocrysts, are termed olivine-rich Al-chondrules. Most of the chondrules we studied are of the olivine-rich variety. There is a third group of Al-chondrules that do not plot on the main Al-chondrule trend noted above (Fig. 2). The three members of this outlier group lie distinctly to the calcium-poor side of the main trend and in two cases essentially plot on the corundum-forsterite side of the ternary. All three are characterized by abundant transparent, pink, isotropic, sodium-aluminum-rich and calcium-poor glass that encloses a phenocryst assemblage of olivine, pyroxene, and in one case, spinel. Because of the elevated iron and sodium contents of these three chondrules, the phase relationships in Fig. 2 (notably for minor phases such as cordierite) do not strictly apply. We term this third variety glassy Al-chondrules.

Of the Al-chondrules reported here, Chainpur 1251-14-2 and Chainpur 5674-2-1 fall into the plagioclase-rich group. These two objects (~300 and 500 μm in size, respectively) are dominated by large calcic (An > 90%) plagioclase crystals that are partially replaced by nepheline. The mesostasis in Chainpur 1251-14-2 is a coarse intergrowth of plagioclase and aluminous diopside. Chainpur 5674-2-1 is somewhat more complex: accompanying its large plagioclase crystals are a few blocky to skeletal forsteritic olivine crystals, and interstitial to the olivine and plagioclase is a coarse to fine dendritic intergrowth of olivine + plagioclase + aluminous diopside. There is a small amount of residual glass.

Olivine-rich Al-chondrules studied include Chainpur 1251-14-1, Inman 5652-1-1, Semarkona 4128-3-2, Chainpur 1251-16-2, Krymka 1729-9-1, and Quinyambie 6076-5-2. Chainpur 1251-14-1 (Russell *et al.*, 1996a; their Fig. 1B) is an elliptical porphyritic chondrule (~600 μm), with phenocrysts of olivine and spinel in a groundmass of plagioclase laths, ophitic aluminous diopside, and sparse iron-nickel metal beads. Inman 5652-1-1 (Russell *et al.*, 1996a; their Fig. 1D) is a ~500 μm barred chondrule with skeletal olivine bars cross-cutting subparallel laths of anorthite, giving the chondrule a cross-barred appearance. Interstitial to the feldspar is aluminous diopside. Rare corroded spinel grains are enclosed in olivine and plagioclase. Parts of the chondrule are fragmented, and it is cut by the same veins of terrestrial iron oxide that affect the rest of the meteorite. Semarkona 4128-3-2 is an oval chondrule fragment, ~350 μm in size, with a coarse and poorly developed barred structure. Interstitial to the forsterite bars are small crystals of unusual magnesium-rich anorthite, aluminous diopside, and minor SiO_2-rich glass. Near the center of the chondrule is a single large, rounded crystal of spinel. Chainpur 1251-16-2 is a complex chondrule or chondrule fragment. The ~700 μm chondrule is dominated by one large, blocky, olivine crystal whose margins are severely scalloped and corroded. It is enclosed in a discontinuous outer zone of untwinned enstatite crystals that locally enclose round blebs of Fe-rich olivine (Fo_{68}). Enclosed within the core of the large olivine crystal is a large irregular area of enstatite, zoned olivine grains, and interstitial plagioclase partially replaced by nepheline. It is not clear if this central region in the large olivine crystal is a fragment or simply a re-entrant of the enstatite rim zone that projects into the olivine from the third dimension. Krymka

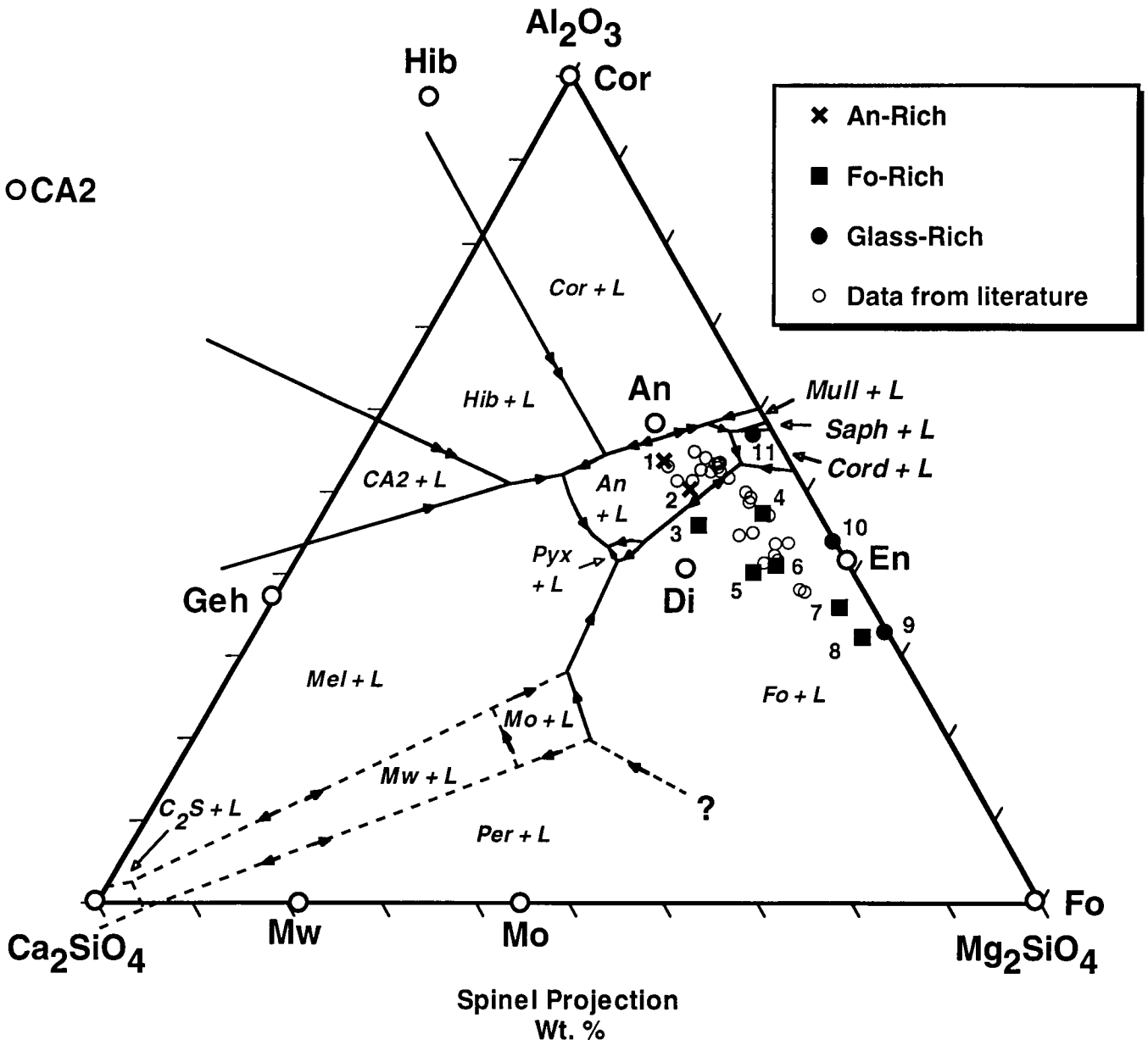

FIG. 2. Bulk compositions of Al-chondrules plotted in the system Al_2O_3–Mg_2SiO_4–Ca_2SiO_4 and projected from spinel ($MgAl_2O_4$). Phase boundaries are spinel-saturated, and are based on experimental data from the literature. The positions of the phase boundaries are strictly valid only for FeO- and Na_2O-free compositions; most of the plotted chondrules have sufficiently low abundances of both components that their presence (if any) significantly affects the crystallization sequences only in the late stages of melt evolution. Mineral abbreviations: An = anorthite, CA2 = $CaAl_4O_7$, Cor = corundum, Cord = cordierite, Di = diopside, Fo = forsterite, Geh = gehlenite, Hib = hibonite, L = liquid, Mel = melilite solid solution, Mull = mullite, Mo = monticellite, Mw = merwinite, Per = periclase, Pyx = pyroxene solid solution, Saph = sapphirine. Al-chondrules from this study are shown in large solid symbols and numbered: 1 = Chainpur 1251-14-2; 2 = Chainpur 1251-2-1; 3 = Inman 5652-1-1; 4 = Quinyambie 6076-5-2; 5 = Chainpur 1251-14-1; 6 = Semarkona 4128-3-2; 7 = Krymka 1729-9-1; 8 = Chainpur 1251-16-2; 9 = Chainpur 1251-3b-1; 10 = Chainpur 1251-16-3; 11 = Chainpur 1251-3-1. Chondrules #1 and #2 plot in the anorthite primary phase field, contain abundant large euhedral plagioclase crystals, and are termed anorthite-rich Al-chondrules. Most POIs of Sheng *et al.* (1991) are anorthite-rich Al-chondrules. Chondrules #3 to #8 plot in the olivine primary phase field, are characterized by large olivine (±spinel) crystals, and are termed olivine-rich Al-chondrules. Chondrules #9 to #11 plot on or near the forsterite-corundum bounding join, are characterized by abundant glass that is iron-bearing and sodium-rich, and are termed glassy Al-chondrules. Literature data for Al-chondrules are from Bishoff and Keil (1983) and Sheng *et al.* (1991). Components are calculated as follows: $Ca_2SiO_4 = 172.24 \times (0.5 \times CaO)$; $Mg_2SiO_4 = 140.69 \times (SiO_2 - 0.5 \times CaO)$; $Al_2O_3 = 101.96 \times (Al_2O_3 + 2 \times SiO_2 - MgO - CaO)$; $MgAl_2O_4 = 142.27 \times (CaO + MgO - 2 \times SiO_2)$. For ternary coordinates as shown in the figure, divide each of the three components that define the ternary plane by their sum (Al_2O_3 + Mg_2SiO_4 + Ca_2SiO_4).

TABLE 1. Magnesium isotopic data for CAIs and Al-rich chondrules.*

	$^{25}Mg/^{24}Mg$†	$^{26}Mg/^{24}Mg$†	F_{Mg}‡	$\delta^{26}Mg$§	$^{27}Al/^{24}Mg$
Semarkona 4128-3-1 melilite-spinel CAI with sodalite					
Pyr #1	0.12662(15)	0.14074(47)	−0.1(1.2)	−1.2(2.2)	0.803(41)
Pyr #2	–	–	–	1.5(1.6)	0.525(29)
Mel #1	0.12673(27)	0.13994(38)	0.8(2.2)	1.0(4.4)	12.5(0.6)
Mel #2	0.12662(40)	0.14064(56)	−0.1(3.2)	7.8(6.0)	16.0(0.8)
Mel #3	0.12701(20)	0.14142(30)	3.0(1.6)	7.2(2.9)	14.8(0.7)
Sod #1	–	–	–	9.0(3.8)	16.9(0.8)
Sod #2	–	–	–	6.9(2.0)	13.6(0.7)
Sod #3	–	–	–	7.5(2.2)	14.3(0.7)
Sod #4	–	–	–	4.8(3.8)	10.4(0.8)
Sod #5	–	–	–	5.8(3.0)	15.4(0.8)
Semarkona 1805-2-1 hibonite-melilite-perovskite-spinel CAI					
Sp #1	0.12675(19)	0.14009(38)	1.0(1.5)	2.0(1.6)	3.7(0.2)
Sp #2	0.12627(25)	0.13907(48)	−2.8(2.0)	2.4(2.5)	2.5(0.2)
Sp #3	0.12650(26)	0.13926(47)	−1.0(2.0)	0.1(2.5)	2.9(0.2)
Mel #1	0.12726(16)	0.14218(24)	5.0(1.3)	8.9(2.4)	18.9(1.0)
Mel #2	0.12723(13)	0.14182(21)	4.8(1.0)	7.0(1.5)	14.2(0.7)
Mel #3	0.12770(26)	0.14287(30)	8.4(2.1)	6.8(4.2)	17.5(0.9)
Mel #4	0.12750(49)	0.14285(51)	6.8(3.9)	9.7(8.1)	32.5(1.8)
Mel #5	0.12684(29)	0.14153(37)	1.7(2.3)	10.7(4.5)	21.2(1.1)
Mel #6	0.12724(23)	0.14151(32)	4.8(1.8)	4.3(3.3)	12.5(0.6)
Quinyambie 6076-5-1 melilite-spinel-perovskite-hibonite CAI					
Sp #1	0.12706(33)	0.14045(66)	3.4(2.6)	−0.4(2.7)	1.7(0.1)
Sp #2	0.12714(33)	0.14062(66)	4.0(2.6)	−0.4(2.8)	3.2(0.2)
Sp #3	0.12721(32)	0.14096(66)	4.6(2.5)	0.9(2.3)	2.1(0.1)
Mel #1	0.12699(12)	0.14051(20)	2.9(0.9)	1.1(1.5)	3.6(0.2)
Mel #2	0.12713(24)	0.14168(29)	3.9(1.9)	7.0(3.9)	21.2(1.1)
Mel #3	0.12738(17)	0.14160(24)	5.9(1.4)	2.8(2.6)	9.8(0.6)
Mel #4	0.12706(23)	0.14127(26)	3.4(1.8)	5.3(3.8)	25.0(1.3)
Mel #10	0.12760(34)	0.14458(37)	7.6(2.7)	20.7(5.8)	51.9(2.6)
Moorabie 6302-2-1 hibonite-spinel-perovskite CAI					
Sp #1	0.12707(25)	0.14057(46)	3.5(1.9)	0.4(1.2)	3.5(0.2)
Sp #2	0.12706(35)	0.14047(67)	3.4(2.8)	−0.1(2.0)	3.3(0.2)
Hib #1	0.12664(22)	0.14159(16)	0.0(1.7)	13.9(1.9)	36.7(1.8)
Hib #2	0.12657(18)	0.14054(16)	−0.5(1.4)	8.1(1.5)	27.8(1.4)
Chainpur 1251-16-3 olivine-pyroxene-glass chondrule					
Oliv #1	0.12636(15)	0.13904(16)	−2.1(1.2)	0.7(2.3)	0.00042(1)
Oliv #2	0.12631(15)	0.13901(16)	−2.6(1.2)	1.3(2.3)	0.00051(1)
Oliv #3	0.12643(15)	0.13907(16)	−1.6(1.2)	−0.2(2.4)	0.00057(1)
Oliv #4	0.12635(15)	0.13890(16)	−2.3(1.2)	−0.1(2.4)	0.00027(1)
Pyr #1	0.12666(14)	0.13955(23)	0.2(1.1)	−0.5(1.7)	0.218(2)
Pyr #2	0.12673(14)	0.13957(23)	0.8(1.1)	−1.4(1.8)	0.374(1)
Gl #1	0.12707(36)	0.14000(52)	3.5(2.8)	−3.7(4.8)	266(13)
Gl #2	0.12647(25)	0.13941(45)	−1.2(2.0)	0.5(2.3)	143.2(7.2)
Gl #3	0.12703(17)	0.14034(30)	3.1(1.3)	−0.3(1.5)	110.4(5.5)
Gl #4	0.12671(52)	0.13945(100)	0.6(4.1)	−1.9(4.7)	53.0(0.9)
Chainpur 5674-3b-1 olivine-glass chondrule					
Oliv #1	–	–	–	−0.6(1.7)	0.15(1)
Gl #1	0.12655(29)	0.13937(53)	−0.6(2.3)	−0.0(3.0)	64(5)
Gl #2	0.12665(31)	0.13992(45)	0.1(2.5)	1.3(4.6)	253(14)
Gl #3	0.12709(20)	0.14086(30)	3.7(1.6)	2.2(2.9)	312(16)
Gl #4	0.12708(36)	0.14071(51)	3.5(2.8)	2.0(5.0)	410(21)
Gl #5	0.12654(28)	0.14011(36)	−0.7(2.2)	5.4(4.3)	493(26)
Gl #6	0.12700(37)	0.14036(44)	2.9(2.9)	−0.2(5.9)	581(30)
Gl #7	0.12674(40)	0.13928(71)	0.8(3.1)	−3.0(4.2)	433(22)
Gl #8	0.12672(31)	0.13961(58)	0.7(2.5)	−0.6(2.9)	278(14)
Chainpur 1251-3-1 olivine-pyroxene-spinel-glass chondrule					
Oliv #1	–	–	–	−0.5(1.5)	0.00148(8)
Oliv #2	0.12710(9)	0.14057(14)	3.7(0.7)	−0.1(1.4)	0.00162(8)
Oliv #3	0.12699(9)	0.14027(13)	2.8(0.7)	−0.5(1.4)	0.00165(9)
Sp #1	0.12730(33)	0.14057(68)	5.3(2.6)	−1.5(2.1)	2.5(0.1)
Sp #2	0.12721(32)	0.14054(68)	4.6(2.5)	−0.3(1.9)	2.5(0.1)
Sp #3	0.12732(30)	0.14081(65)	5.5(2.4)	−1.9(1.7)	2.6(0.1)
Sp #4	0.12731(30)	0.14089(65)	5.4(2.1)	−1.1(1.3)	2.5(0.1)
Sp #5	0.12741(31)	0.14126(65)	6.1(2.4)	−0.1(1.7)	2.5(0.1)
Sp #6	0.12794(32)	0.14225(66)	10.3(2.5)	−1.3(2.1)	2.5(0.1)
Sp #7	0.12742(31)	0.14125(65)	6.2(2.4)	−0.2(1.8)	2.5(0.1)
Gl #1	0.12717(34)	0.14075(67)	4.3(2.7)	1.6(2.9)	53.7(2.7)
Gl #2	0.12728(34)	0.14126(64)	5.2(2.7)	3.7(2.4)	51.0(2.6)
Gl #3	0.12737(35)	0.14117(66)	5.9(2.8)	1.6(2.8)	49.9(2.5)
Gl #4	0.12723(34)	0.14095(62)	4.7(2.7)	2.3(2.3)	44.1(2.2)
Gl #5	0.12699(33)	0.14060(62)	2.8(2.6)	3.6(2.2)	50.6(2.5)

TABLE 1. *Continued.*

	$^{25}Mg/^{24}Mg$†	$^{26}Mg/^{24}Mg$†	F_{Mg}‡	$\delta^{26}Mg$§	$^{27}Al/^{24}Mg$
Chainpur 1251-14-1 olivine-pyroxene-plagioclase chondrule					
Oliv #1	0.12634(51)	0.13896(111)	−2.3(4.0)	0.0(1.7)	0.0090(6)
Oliv #2	0.12633(51)	0.13899(111)	−2.3(4.0)	0.8(1.9)	0.00073(4)
Oliv #3	0.12640(51)	0.13915(111)	−1.8(4.0)	0.7(1.9)	0.0034(2)
Plag #1	0.12603(125)	0.13893(241)	−5(10)	5(12)	123.3(7.3)
Plag #2	0.12670(113)	0.13858(236)	1(9)	−8.0(7.0)	174.4(9.5)
Plag #3	0.12575(86)	0.13798(172)	−7(7)	1.2(5.9)	82.6(4.7)
Plag #4	0.12647(110)	0.13929(234)	−1(9)	0.7(5.2)	37.5(1.9)
Plag #5	0.12640(56)	0.13919(118)	−1.8(4.3)	1.2(3.0)	42.6(2.1)
Plag #6	0.12626(114)	0.13889(236)	−3(9)	1.1(7.7)	61.2(3.1)
Plag #7	0.12662(78)	0.13964(166)	−0.1(6.2)	0.8(3.4)	31.5(1.7)
Chainpur 1251-14-2 plagioclase-diopside chondrule					
Pyr #1	–	–	–	1.1(3.3)	2.8(0.1)
Pyr #2	–	–	–	1.0(1.3)	2.4(0.1)
Pyr #3	–	–	–	−1.1(1.9)	1.1(0.1)
Plag #1	0.12551(90)	0.13797(171)	−8.8(7.1)	6.1(8.8)	69.0(4.0)
Plag #2	0.12621(55)	0.13814(100)	−3.3(4.3)	−2.3(5.6)	130.5(6.7)
Plag #3	0.12631(66)	0.13839(124)	−2.5(5.2)	−4.2(6.1)	166.6(8.7)
Plag #4	0.12686(143)	0.13785(249)	2(11)	−16(17)	210(14)
Plag #5	0.12673(154)	0.13967(276)	1(12)	−1(21)	293(17)
Plag #6	0.12683(156)	0.13948(258)	2(12)	−4(20)	408(22)
Chainpur 1251-16-2 enstatite-diop.-plag.-nepheline-olivine chondrule					
Pyr #1	–	–	–	0.7(1.4)	0.072(4)
Plag #1	0.12660(43)	0.13926(71)	−0.2(3.4)	−1.6(6.7)	47.6(2.5)
Plag #2	0.12655(28)	0.13975(45)	−0.6(2.2)	2.8(4.1)	109.0(5.5)
Plag #3	0.12681(26)	0.13974(44)	1.5(2.1)	−1.5(3.7)	79.3(4.1)
Plag #4	0.12617(22)	0.13883(35)	−3.6(1.8)	2.2(3.1)	139.9(7.0)
Quinyambie 6076-5-2 olivine-pyroxene-plagioclase chondrule					
Pyr #1	–	–	–	0.7(1.5)	0.0048(2)
Pyr #2	–	–	–	0.1(1.4)	0.0130(7)
Pyr #3	–	–	–	−1.1(1.5)	0.0039(4)
Plag #1	0.12608(96)	0.13897(197)	−4.3(4.2)	4.5(6.4)	47.7(2.5)
Plag #2	0.12646(68)	0.13914(143)	−1.2(2.9)	−0.5(3.6)	46.0(2.3)
Plag #3	0.12618(93)	0.13876(197)	−3.6(3.9)	1.5(5.2)	43.5(2.3)
Plag #4	0.12619(90)	0.13864(195)	−3.4(3.4)	0.4(3.5)	37.9(2.1)
Plag #5	0.12647(92)	0.13973(197)	−1.3(3.7)	3.8(4.8)	60.7(3.1)
Plag #6	0.12623(65)	0.13889(138)	−3.0(2.6)	1.2(3.0)	28.1(1.4)
Plag #7	0.12644(92)	0.13931(196)	−1.5(3.7)	1.3(4.7)	83.8(4.2)
Plag #8	0.12634(91)	0.13890(195)	−2.3(3.5)	−0.0(4.1)	64.3(3.2)
Plag #9	0.12653(71)	0.13937(141)	−0.6(3.2)	0.1(4.6)	69.7(3.5)
Chainpur 1251-3-1 olivine-pyroxene-spinel-glass chondrule *(continued)*					
Gl #6	0.12709(33)	0.14090(62)	3.6(2.6)	4.0(2.1)	50.6(2.6)
Gl #7	0.12715(33)	0.14078(62)	4.1(2.6)	2.2(2.1)	50.2(2.5)
Gl #8	0.12703(34)	0.14071(62)	3.1(2.7)	3.7(2.2)	51.7(2.6)
Gl #9	0.12774(44)	0.14198(89)	8.7(3.6)	−0.1(3.6)	58.6(3.0)
Gl #10	0.12767(43)	0.14216(88)	8.2(3.4)	2.2(3.1)	54.3(2.7)
Gl #11	0.12752(42)	0.14196(88)	7.0(3.3)	3.3(2.9)	61.3(3.1)
Gl #12	0.12775(42)	0.14240(88)	8.8(3.3)	2.8(2.6)	55.6(2.8)
Gl #13	0.12761(41)	0.14185(88)	7.7(3.3)	1.0(2.5)	50.8(2.5)
Gl Mean	0.12730(10)	0.14118(20)	5.3(0.8)	2.7(0.7)	51.8(0.7)
Chainpur 5674-2-1 plagioclase-olivine-pyroxene chondrule					
Oliv #1	0.12661(23)	0.13961(46)	−0.2(1.8)	0.8(1.9)	0.209(17)
Oliv #2	0.12677(22)	0.13991(45)	1.1(1.7)	0.5(1.5)	0.0099(12)
Oliv #3	0.12686(21)	0.13995(45)	1.8(1.7)	−0.6(1.2)	0.148(20)
Pyr #1	–	–	–	1.6(1.7)	1.00(6)
Pyr #2	–	–	–	−1.0(1.4)	0.54(3)
Plag #1	0.12652(102)	0.13966(202)	−0.8(5.1)	2.5(8.9)	298(15)
Plag #2	0.12668(98)	0.13964(201)	0.3(4.5)	−0.1(7.6)	219(11)
Plag #3	0.12639(101)	0.13886(201)	−1.9(4.9)	−1.1(8.6)	90.5(4.8)
Plag #4	0.12670(65)	0.13988(139)	0.6(5.2)	1.0(3.1)	87.6(4.4)
Plag #5	0.12679(65)	0.14029(140)	1.2(5.2)	2.1(3.2)	86.0(4.3)
Plag #6	0.12675(92)	0.14009(197)	1.0(3.5)	1.9(4.1)	63.6(3.3)
Nep #1	–	–	–	−5.3(9.1)	533(29)
Semarkona 4128-3-2 plagioclase-olivine-spinel chondrule					
Oliv #1	0.12657(15)	0.13954(19)	−0.5(1.2)	0.9(2.4)	0.0369(49)
Oliv #2	0.12658(11)	0.13928(13)	−0.4(0.9)	−1.2(1.5)	0.1020(72)
Oliv #3	0.12650(11)	0.13923(14)	−1.1(0.9)	−0.2(1.6)	0.0033(2)
Sp #1	0.12677(23)	0.14002(13)	1.1(1.8)	1.1(1.3)	2.5(0.1)
Sp #2	0.12688(17)	0.13996(12)	1.9(1.4)	−0.8(1.5)	2.4(0.1)
Sp #3	0.12694(24)	0.14005(48)	2.5(1.9)	−1.3(1.8)	2.5(0.2)
Plag #1	0.12663(15)	0.13978(19)	0.0(1.2)	2.0(2.7)	29.0(1.5)
Plag #2	0.12694(29)	0.14021(35)	2.5(2.3)	−0.0(5.1)	26.4(1.3)
Plag #3	0.12683(32)	0.13974(35)	1.6(2.5)	−1.6(5.4)	15.5(0.9)
Plag #4	0.12632(39)	0.13933(45)	−2.5(3.1)	3.6 ± 6.8	29.5(1.5)
Plag #5	0.12670(25)	0.13992(33)	0.5(2.0)	1.9 ± 4.3	27.2(1.4)
Plag #6	0.12651(31)	0.13897(42)	−1.0(2.4)	−2.0 ± 5.5	29.2(1.5)
Plag #7	0.12656(41)	0.13946(72)	−0.5(3.2)	0.1 ± 2.7	12.9(0.7)
Plag #8	0.12647(37)	0.13923(52)	−1.3(2.9)	0.9 ± 4.9	20.1(1.0)
Plag #9	0.12617(34)	0.13906(58)	−3.7(2.7)	3.7 ± 4.0	27.9(1.4)
Plag #10	0.12634(57)	0.13876(100)	−2.3(4.5)	−1.1 ± 6.1	17.9(1.5)
Plag #11	0.12663(35)	0.13926(58)	0.0(2.8)	−1.4 ± 4.1	22.1(1.1)

TABLE 1. *Continued.*

	$^{25}Mg/^{24}Mg$†	$^{26}Mg/^{24}Mg$†	F_{Mg}‡	$\delta^{26}Mg$§	$^{27}Al/^{24}Mg$		$^{25}Mg/^{24}Mg$†	$^{26}Mg/^{24}Mg$†	F_{Mg}‡	$\delta^{26}Mg$§	$^{27}Al/^{24}Mg$
Inman 5652-1-1 barred-olivine-plagioclase chondrule						**Krymka 1729-9-1 olivine-pyroxene-plagioclase chondrule**					
Oliv #1	0.12685(22)	0.14018(46)	1.8(1.7)	1.0(1.6)	0.0123(6)	Oliv #1	0.12693(24)	0.14043(46)	2.4(1.9)	1.5(2.2)	0.0067(3)
Oliv #2	0.12681(22)	0.14011(46)	1.4(1.7)	1.2(1.6)	0.0040(2)	Oliv #2	0.12667(23)	0.13951(48)	0.3(1.3)	–0.9(2.1)	0.0223(20)
Oliv #3	0.12715(22)	0.14067(46)	4.1(1.8)	–0.2(1.8)	0.0065(4)	Oliv #3	0.12679(23)	0.13987(46)	1.3(1.8)	–0.3(2.0)	0.0024(1)
Plag #1	0.12663(43)	0.14055(86)	0.5(3.2)	5.0(3.9)	35.5(1.8)	Oliv #4	0.12684(24)	0.13993(46)	1.7(1.9)	–0.6(2.4)	0.0024(1)
Plag #2	0.12678(58)	0.13982(118)	1.4(3.5)	1.1(3.8)	27.4(1.4)	Plag #1	0.12667(54)	0.13994(114)	0.3(2.3)	2.2(3.0)	41.9(2.1)
Plag #3	0.12678(53)	0.14029(115)	0.9(3.3)	2.9(2.8)	31.5(1.7)	Plag #2	0.12648(52)	0.13973(101)	–1.2(2.6)	3.1(4.7)	70.7(3.5)
Plag #4	0.12588(45)	0.13797(97)	–5.6(3.1)	1.2(1.7)	12.4(0.6)	Plag #3	0.12697(98)	0.14029(200)	2.7(4.4)	0.0(7.1)	92.0(4.7)
Plag #5	0.12734(53)	0.14233(95)	6.1(4.1)	8.7(5.9)	77.2(3.9)	Plag #4	0.12662(74)	0.13930(143)	0.0(3.8)	–2.0(6.8)	67.3(3.4)
Plag #6	0.12704(66)	0.14052(140)	3.3(3.3)	0.8(3.3)	20.4(1.0)	Plag #5	0.12666(57)	0.13972(116)	–0.1(2.6)	2.8(4.2)	72.2(3.6)
						Plag #6	0.12636(57)	0.13914(115)	–2.6(2.6)	3.3(3.9)	65.2(3.3)

*The 2σ errors, in parentheses, refer to the least significant digits.
† $^{25}Mg/^{24}Mg$ and $^{26}Mg/^{24}Mg$ have been corrected for instrumental mass fractionation.
‡ F_{Mg} was calculated from $^{25}Mg/^{24}Mg$ after correction for instrumental mass fractionation.
§ $\delta^{26}Mg$ was calculated without making a separate correction for instrumental mass fractionation. $^{26}Mg^*$ is the excess after accounting for all types of mass fractionation.
Abbreviations: Pyr = pyroxene, Mel = melilite, Sod = sodalite, Sp = spinel, Hib = hibonite, Oliv = olivine, Plag = plagioclase, Gl = glass, Nep = nepheline.

1729-9-1 (Russell *et al.*, 1996a) is a 1 mm diameter granular chondrule consisting mostly of blocky olivine grains with minor interstitial calcic plagioclase, rare metal grains, pigeonite (exsolved), and ilmenite. Small enstatite grains occur around the periphery of the chondrule. Quinyambie 6076-5-2 (called Moorabie 6076-5-2 in Russell *et al.*, 1996a; Fig. 1 in Russell *et al.*, 2000) is an incomplete rounded chondrule (at least ~575 μm in diameter) that is composed of blocky olivine crystals partially enclosed within subcalcic augite. Interstitial to these are partly maskelynitized plagioclase crystals.

Three glassy Al-chondrules were analyzed: Chainpur 1251-3-1 (Fig. 1C in Russell *et al.*, 1996a), Chainpur 1251-16-3, and Chainpur 5674-3b-1. Chainpur 1251-3-1 is a broken, originally spherical, porphyritic chondrule (~850 μm in diameter). Spinel and olivine crystals are set in a mesostasis of dendritic aluminous diopside and pink, sodium-rich glass. Small pyroxene crystals at the chondrule rim contain cores of pigeonite. Chainpur 1251-16-3 is a ~450 μm, barred chondrule with two sets of magnesium-rich olivine bars set in pink, isotropic glass. The chondrule margin has a discontinuous shell of olivine. A few small skeletal pyroxene crystals are scattered in the glass and consist of pigeonite cores rimmed by aluminous diopside. A large metal-troilite nodule and small (~10 μm) metal spheres are also present. Chainpur 5674-3b-1 is an ~850 μm, compound chondrule. Part of it consists of densely packed equant olivine crystals and abundant metal and sulfide blebs imbedded in pink, isotropic glass. Enclosed within this porphyritic region is half of a barred-olivine chondrule that was originally ~400 μm in diameter. Interstitial to the olivine bars is pink, isotropic glass. The barred portion is nearly metal and sulfide free.

Aluminum-Magnesium Isotope Systematics

Magnesium isotopic data and aluminum-magnesium ratios for the four CAIs and eleven chondrules are presented in Table 1 and in Figs. 3–7.

Calcium-Aluminum-Rich Inclusions–All of the CAIs analyzed exhibit clear aluminum-correlated excesses of $^{26}Mg^*$, with initial ratios ($(^{26}Al/^{27}Al)_0$) indistinguishable from the canonical value of 5×10^{-5} for CAIs from carbonaceous chondrites (Fig. 3). The secondary sodalite in Semarkona 4128-3-1 also contains $^{26}Mg^*$ that is positively correlated with Al/Mg, giving the same $(^{26}Al/^{27}Al)_0$ as the primary minerals (Fig. 3a). This is significant because feldspathoids in CAIs only rarely show $^{26}Mg^*$ (Brigham *et al.*, 1986; also see review in MacPherson *et al.*, 1995). Hence, the data for 4128-3-1 may indicate that the secondary alteration took place very soon after the formation of the CAI.

Three out of the four CAIs exhibit small intrinsic mass-dependent fractionation effects in magnesium (Table 1). In Quinyambie 6076-5-1 both spinel and melilite are enriched in the heavy isotopes (weighted mean $F_{Mg} \approx +4‰$/amu). Spinel in Semarkona 1805-2-1 is essentially unfractionated while

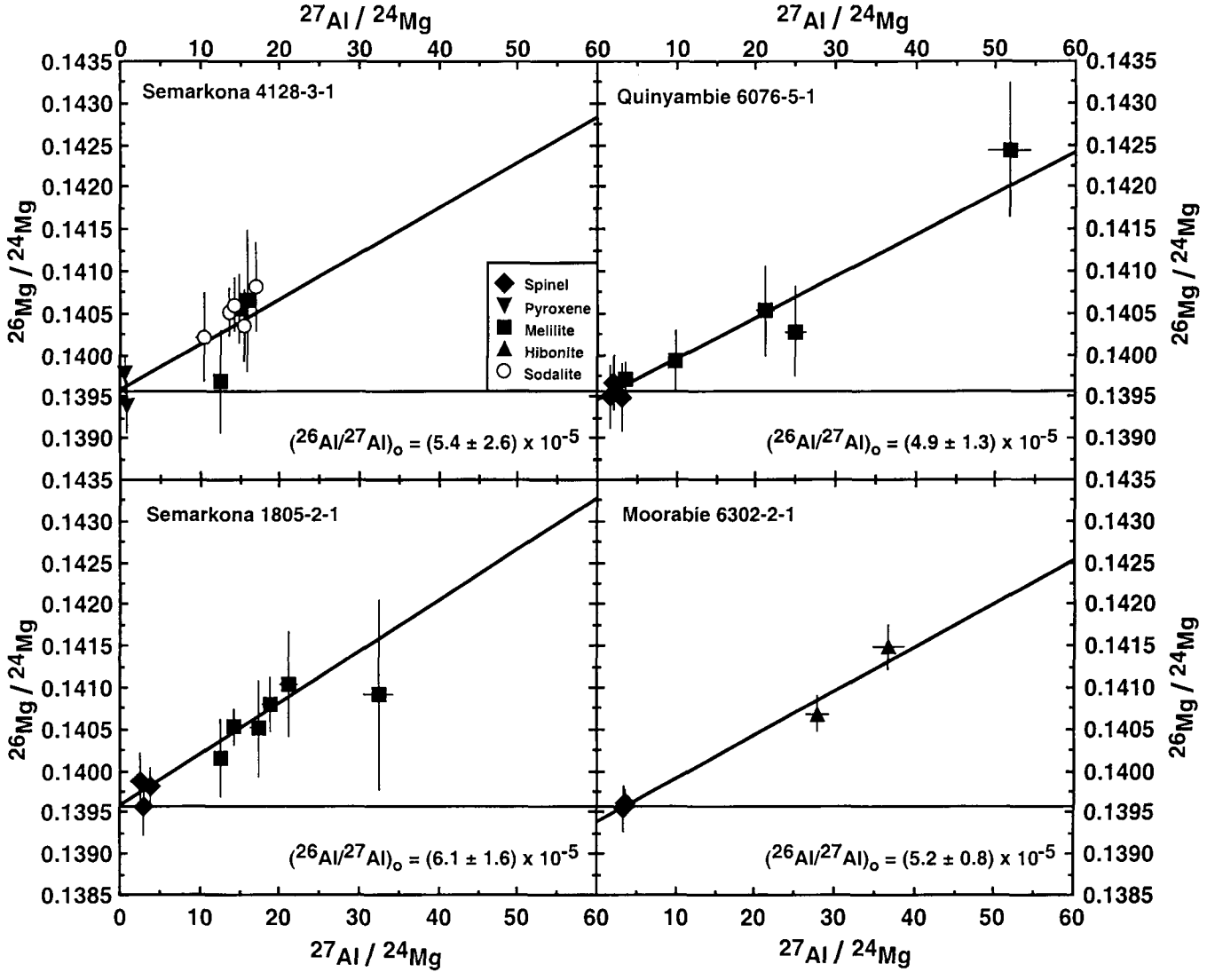

FIG. 3. Magnesium evolution diagram for CAIs in this study. In this diagram, phases that have co-crystallized in the presence of ^{26}Al and have remained undisturbed will lie on a straight line with a positive slope. The slope of the line gives the initial $^{26}Al/^{27}Al$ ratio ($(^{26}Al/^{27}Al)_0$) and the intercept gives the initial $^{26}Mg/^{24}Mg$ ratio. The horizontal line on each panel gives the $^{26}Mg/^{24}Mg$ ratio measured in the standard minerals. All four of the CAIs exhibit clear evidence of ^{26}Al and the inferred $(^{26}Al/^{27}Al)_0$ ratios lie within errors of the canonical value for the early solar system ($\sim 5 \times 10^{-5}$). The precision of the estimates of $(^{26}Al/^{27}Al)_0$ is relatively low because the low $^{27}Al/^{24}Mg$ ratios for the measured minerals, particularly for the Semarkona inclusions, do not provide much leverage to determine the slope of the line. Errors on data points and on inferred slopes are 2σ. Data for Semarkona 1805-2-1 and Quinyambie 6076-5-1 from Russell *et al.* (1996a).

melilite is enriched in heavy isotopes ($F_{Mg} \approx +5$‰/amu). In Moorabie 6302-2-1, hibonite is unfractionated, in contrast to spinel, which is isotopically slightly heavy ($F_{Mg} \approx +3.5$‰/amu). In Semarkona 4128-3-1, pyroxene and two of three measured melilites are essentially unfractionated but a third melilite appears to be fractionated by $F_{Mg} \approx +3$‰/amu. However, the weighted mean for the melilite analyses is $F_{Mg} \approx +1.9$‰/amu, which we do not consider resolved from zero. We emphasize that uncertainties for the individual fractionation measurements are large, so caution should be taken in interpreting the fractionation differences between phases in individual inclusions.

Chondrules–Of the eleven Al-chondrules measured in this study, only two show clear evidence of $^{26}Mg^*$ (Fig. 4). In Inman 5652-1-1, the most aluminum-rich plagioclase crystals show clearly resolved $^{26}Mg^*$ corresponding to $(^{26}Al/^{27}Al)_0 \approx 1 \times 10^{-5}$, a factor of 5 lower than the ratio common to many CAIs. In Chainpur 1251-3-1, sodium-rich glass exhibits excess $^{26}Mg^*$ relative to spinel and olivine. Although the excess for each individual ion probe measurement is comparable to the 2σ uncertainty for that measurement, the weighted mean of $^{26}Mg/^{24}Mg$ for 13 measurements is resolved from normal magnesium by almost 8σ (Fig. 5). The inferred $(^{26}Al/^{27}Al)_0$ for this chondrule, $\sim 9 \times 10^{-6}$, is again ~5× lower those inferred for most CAIs.

None of the other nine Al-chondrules in this study shows clear evidence for $^{26}Mg^*$ (Figs. 6 and 7). In Russell *et al.*

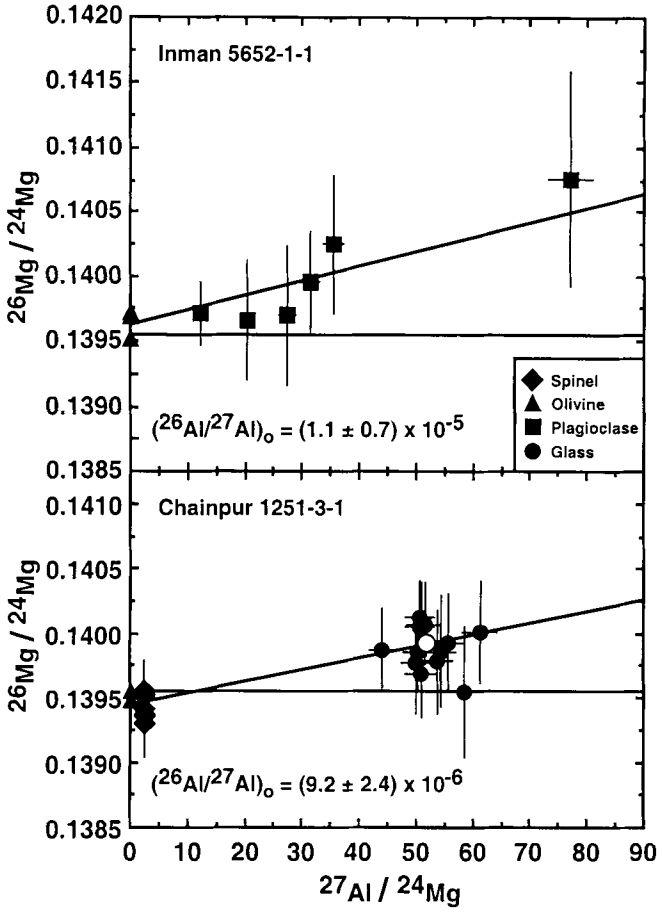

FIG. 4. Magnesium evolution diagram for the two Al-chondrules with evidence for ^{26}Al. For Inman 5652-1-1, the two measurements for plagioclase with the highest $^{27}Al/^{24}Mg$ ratio show clearly resolved excesses of radiogenic $^{26}Mg^*$ and the data are consistent with a single array of slope $(^{26}Al/^{27}Al)_0 = (1.1 \pm 0.7) \times 10^{-5}$. For Chainpur 1251-3-1, the individual measurements for glass are not clearly resolved from normal Mg, but the mean of thirteen measurements is resolved by almost 8σ. The line generated by a weighted least-squares fit of the olivine, spinel, and glass data has a slope of $(^{26}Al/^{27}Al)_0 = (9.2 \pm 2.4) \times 10^{-6}$. Data from Russell *et al.* (1996a).

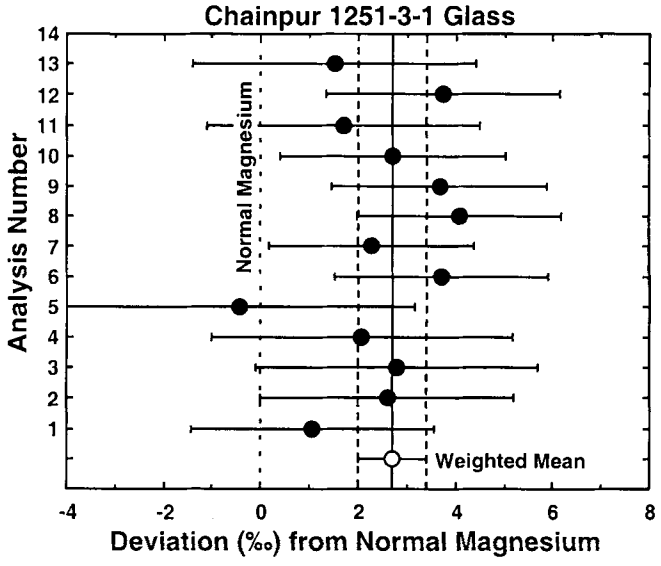

FIG. 5. The individual fractionation-corrected $^{26}Mg/^{24}Mg$ measurements for glass in Chainpur 1251-3-1 are compared with normal Mg (dotted line) and with the regression line shown in Fig. 4 (solid line). Although most of the individual measurements are not resolved at the 2σ level from normal Mg, the weighted mean of the analyses is resolved by nearly 8σ (dashed lines show the 2σ uncertainty in the mean). Data from Russell *et al.* (1996a).

(1997), a detection of $^{26}Mg^*$ in Semarkona 4128-3-2 was reported with $(^{26}Al/^{27}Al)_0$ of ~2.4×10^{-5}. However, after additional repeated measurements, we were unable to confirm this value. The present more-extensive data set can only place an upper limit on $(^{26}Al/^{27}Al)_0$ of $<1.7 \times 10^{-5}$ (Fig. 7). This upper limit is consistent with initial ratios determined for other Semarkona chondrules of $(0.5–1) \times 10^{-5}$ (Kita *et al.*, 2000; McKeegan *et al.*, 2000). The limits that can be placed on $(^{26}Al/^{27}Al)_0$ depend on the Al/Mg ratio in the high Al phases and the precision of the isotope analysis. Limits on $(^{26}Al/^{27}Al)_0$ range from $<1.7 \times 10^{-5}$ for Semarkona 4128-3-2 to $<1 \times 10^{-6}$ for several Chainpur chondrules (Figs. 6 and 7).

Only one Al-chondrule shows significant evidence for mass-dependent fractionation in magnesium, Chainpur 1251-3-1 (Table 1). Olivine, spinel, and glass all appear to be isotopically heavy, with weighted means for F_{Mg} ranging from about +3‰/amu (olivine) to about +5‰/amu and +6‰/amu (glass and spinel, respectively). This is comparable in both sign and degree to the mass fractionations observed in CAIs and indicates significant evaporative loss of magnesium from a melt. None of the other chondrules shows clear evidence of mass fractionation, although fractionations of 1–2‰/amu would not be resolved by our data.

DISCUSSION

Although nearly 25 years have past since clear evidence was reported for live ^{26}Al in the early solar system, there is still no consensus on how widely ^{26}Al was distributed or whether it can be used as a relative chronometer of early solar system events. For many years, evidence for ^{26}Al in the early solar system was confined almost entirely to CAIs from carbonaceous (C) chondrites. Recent work, including this study, has now expanded the database to include CAIs from ordinary and enstatite (E) chondrites and to include Al-chondrules and ferromagnesian chondrules from C and O chondrites. In the following discussion, we first compare the ^{26}Al data for CAIs from UOCs with equivalent data for CAIs from E and C chondrites and discuss the implications for the primordial distribution of ^{26}Al. We then compare the chondrule data. Next, we use the combined data sets to assess the status of ^{26}Al as a chronometer. Finally, assuming that it can be used as a chronometer, we summarize constraints provided by ^{26}Al on the timing of events in the early solar system. To aid the discussion, we have compiled our data

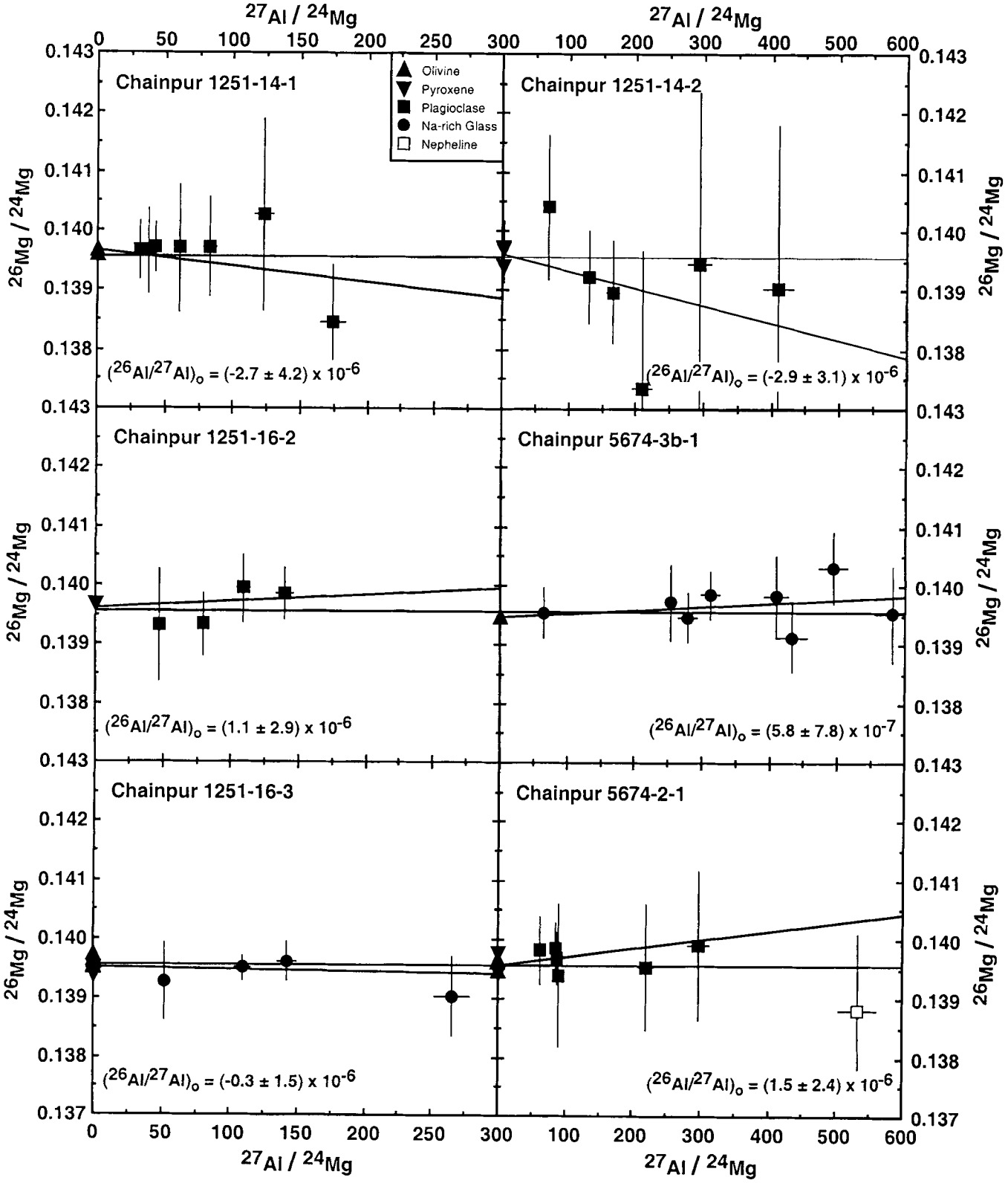

FIG. 6. Magnesium evolution diagram for Al-chondrules from Chainpur. None of these six chondrules exhibits any evidence for the presence of $^{26}Mg^*$, but the limits on $(^{26}Al/^{27}Al)_0$ permitted by the data are, in most cases, not particularly tight. For example, Chainpur 5674-2-1 exhibits an array with a positive slope of ~1 × 10^{-6}, with large errors. This sample could have had a $(^{26}Al/^{27}Al)_0$ ratio similar to those for chondrules in Semarkona. The array for this chondrule was calculated without the secondary nepheline, which would have constrained $(^{26}Al/^{27}Al)_0$ to be considerable lower.

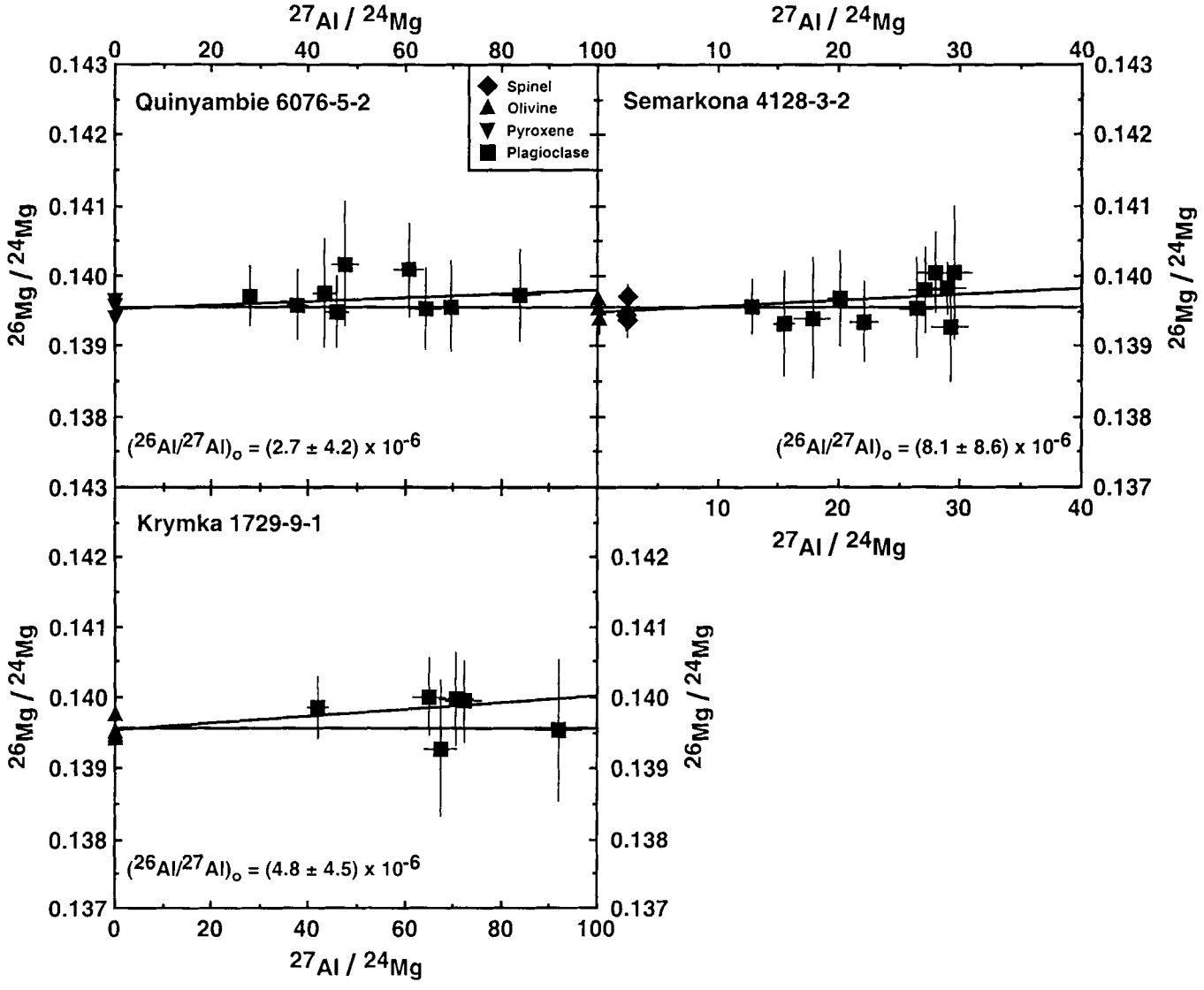

FIG. 7. Magnesium evolution diagram for three Al-chondrules with no evidence for $^{26}Mg^*$. As with the Chainpur chondrules in Fig. 6, the constraints on $(^{26}Al/^{27}Al)_0$ provided by the data are not particularly tight. All three chondrules could have contained ^{26}Al at a level of $(^{26}Al/^{27}Al)_0$ = a few $\times 10^{-6}$ to 1×10^{-5}.

together with the published aluminum-magnesium data for CAIs, chondrules, and other $^{26}Mg^*$-bearing objects from UOCs in Table 2, and we have plotted the data for UOCs in Fig 8. Table 2 also summarizes the published data for Al-chondrules from C chondrites (the voluminous data for CAIs are not given; see review by MacPherson *et al.*, 1995).

Aluminum-26 in Calcium-Aluminum-Rich Inclusions

The majority of the evidence for live ^{26}Al in the early solar system comes from CAIs, which are most abundant in CM, CV, and CO chondrites. Most of these formed with $(^{26}Al/^{27}Al)_0$ of 4×10^{-5} to 5×10^{-5}, and the latter value is now commonly accepted as "canonical" for the early solar system. The bulk of the data come from two meteorites—Allende (CV) and Murchison (CM)—and represents a wide diversity of CAI types (reviewed by MacPherson *et al.*, 1995). The recent discovery that most CAIs in UOCs contained ^{26}Al when they formed (Russell *et al.*, 1996a; this paper), together with a similar finding for CAIs in unequilibrated enstatite (E3) chondrites (Guan *et al.*, 2000a), changed this picture. CAIs with $(^{26}Al/^{27}Al)_0 \approx 5 \times 10^{-5}$ have now been found in almost all of the major chondrite classes (CM, CO, CV, CR, CH, O, E). The current database, which includes data for inclusions with different mineral assemblages and for inclusions from meteorites of different petrologic type, allows us to discriminate between original isotopic features present when the inclusions formed and those isotopic properties resulting from secondary processes. The combined data place constraints on the timing of secondary alteration of CAIs, both before and after accretion

into the meteorite parent bodies, and may constrain the time of final accretion of the meteorite parent bodies.

There are now six CAIs from UOCs for which aluminum-magnesium data have been obtained, including the two reported in Russell *et al.* (1996a) and the two new ones reported here (Table 2). The precision obtained on these small fragments is often lower than that which can be obtained from large CAIs in CV chondrites. Nonetheless, four of the CAIs from UOCs show $(^{26}Al/^{27}Al)_0$ compatible with the canonical value of $\sim 5 \times 10^{-5}$ (Fig. 3). Two others show distinctly lower values. In particular, the first CAI identified in a UOC, Dhajala DH-H1 (a hibonite fragment), gave a well-defined isochron with $(^{26}Al/^{27}Al)_0 = 8.4 \times 10^{-6}$ (Hinton and Bischoff, 1984). This initial ratio was confirmed by Ireland *et al.* (1992), who also showed that DH-H1 is a FUN inclusion with mass-fractionated calcium and titanium and a ~6‰ deficit (intrinsic nuclear anomaly) at ^{48}Ca. The second inclusion shows no evidence of ^{26}Al; it is a plagioclase-bearing CAI from Clovis (H3.9) (Hutcheon *et al.*, 1994). Clovis likely experienced a peak metamorphic temperature of ~650–700 °C (Wlotzka, 1985), which is capable of isotopically resetting plagioclase in $\sim 10^5$ years (LaTourrette and Wasserburg, 1998). Thus, metamorphic resetting is likely. Dhajala (3.8) was heated too, probably to ~600–650 °C, but the evidence for ^{26}Al in DH-H1 is contained in hibonite, a mineral that is resistant to metamorphism. For example, hibonite in CO3 chondrites of all petrologic subtypes retains $^{26}Mg^*$ (Russell *et al.*, 1998), even in meteorites that experienced temperatures of up to 600 °C for extended periods (cf., Sears *et al.*, 1991b). Also, the hibonite-rich inclusion from Moorabie, another 3.8 chondrite, still exhibits a good isochron (Fig. 3d). This suggests that magnesium isotopic reequilibration in the parent body is not responsible for the low $(^{26}Al/^{27}Al)_0$ inferred for DH-H1.

CAIs from E3 chondrites also incorporated live ^{26}Al (Guan *et al.*, 2000a). Seven of eleven small hibonite-bearing CAIs from three E chondrites measured by Guan *et al.* (2000a) exhibit $(^{26}Al/^{27}Al)_0$ ratios at or near the canonical value of $\sim 5 \times 10^{-5}$. For the other four CAIs, upper limits range between 0.25×10^{-5} and 1×10^{-5}. All eleven inclusions are hibonite-bearing, and two of the three E chondrites contain inclusions both with and without evidence of ^{26}Al. Therefore, as in the case of UOCs, metamorphism of the E chondrites probably does not explain the low initial values in some of their CAIs.

Thus, most CAIs from UOC and E chondrites apparently formed with similar initial $^{26}Al/^{27}Al$ values of $\sim 5 \times 10^{-5}$, the canonical value originally established by the C-chondrite CAIs. And, as with C-chondrite CAIs (Wasserburg *et al.*, 1977), rare CAIs in UOC and E chondrites formed with much lower or no detectable initial $^{26}Al/^{27}Al$. CAIs in the three chondrite classes have other similarities besides their $(^{26}Al/^{27}Al)_0$ systematics. To a first approximation, CAIs from UOC and E chondrites have direct petrologic analogues in C chondrites (neglecting such differences as size distributions and alteration histories; for example, Guan *et al.*, 2000a; Fagan *et al.*, 2000). CAIs from the different chondrite groups even have similar oxygen isotopic compositions (McKeegan *et al.*, 1998; Guan *et al.*, 2000b,c; Fagan *et al.*, 2001). These petrologic and isotopic similarities in CAIs from C, O, and E chondrites could imply that CAIs formed *via* a general process that operated throughout all the chondrite-accretion zones on a nebula-wide, uniform isotopic reservoir. If so, the signature of $(^{26}Al/^{27}Al)_0 \approx 5 \times 10^{-5}$ would indicate most CAIs formed at approximately the same time and that lower ratios reflect later formation times or reprocessing. Alternatively, the uniformity of isotopic systematics might imply that most CAIs formed in a restricted region in the solar system and were later dispersed throughout the various chondrite-accretion zones (*e.g.*, McKeegan *et al.*, 1998; Guan *et al.*, 2000a,c; Shu *et al.*, 1996). In this case the direct evidence for a nebula-wide $(^{26}Al/^{27}Al)_0 \approx 5 \times 10^{-5}$ largely disappears because that signature is uniquely associated with CAIs assumed to have formed in only one region of the solar nebula. However, even in this model the inferred $(^{26}Al/^{27}Al)_0$ values would constrain formation times if ^{26}Al was brought in with nebular dust and seeded homogeneously throughout the early solar system. Only if both the ^{26}Al and the CAIs were produced in the same restricted region would variations in ^{26}Al abundance between CAIs and other chondritic material carry no time information.

Mineralogy and textural relationships show that most CAIs have had complex histories (*e.g.*, review by MacPherson *et al.*, 1988). Some show clear evidence of multiple melting events that apparently occurred over extended periods of time. These textural sequences can be reflected in the ^{26}Al results. For example, Allende CAI 5241 has three distinct petrologic units, a spinel-rich core, spinel-free islands, and a melilite mantle. Each of these units gives a different ^{26}Al isochron, the slopes of which (initial ratios) range from 3.3×10^{-5} to $\sim 5 \times 10^{-5}$ (Hsu *et al.*, 2000). These initial ratios are consistent with the texturally inferred sequence of events in the CAI and imply an evolutionary history of $\sim 4 \times 10^5$ years for this object. Many inclusions also experienced low-temperature metasomatism. The isotopic signatures of the secondary phases range from $(^{26}Al/^{27}Al)_0 \approx 0$ in some inclusions (*e.g.*, Hutcheon and Newton, 1981) to $\sim 5 \times 10^{-5}$ in others (Brigham *et al.*, 1986; Semarkona 4128-3-1 (Fig. 1a)). Some inclusions even show evidence of partial re-melting after such metasomatic alteration, with the second-generation igneous phases showing no $^{26}Mg^*$ excesses (MacPherson and Davis, 1993). Interpreted in terms of time, the differences in $(^{26}Al/^{27}Al)_0$ imply individual CAI histories of as long as 2 Ma. Of course, an alternate (and somewhat *ad hoc*) interpretation of this data is that after ^{26}Al-rich CAIs formed, they were transported to a location with no ^{26}Al, where the metasomatic events involving chemical and isotopic exchange with the external reservoir produced secondary phases without ^{26}Al. But, even if the secondary phases do not contain time information, the correlation between $(^{26}Al/^{27}Al)_0$ and "primary" melting events like those in Allende 5241 seem to be best interpreted in terms of an extended history

TABLE 2. Summary of ^{26}Al data for aluminum-rich objects from UOCs.

Sample	High-Al Phase	$^{27}Al/^{24}Mg$	$\delta^{26}Mg$ (‰)	$(^{26}Al/^{27}Al)_0 \times 10^{-5}$†	Reference
CAIs					
Semarkona (LL3.0) 1805-2-1	melilite	12–33	4.3–10.7	**6.1 ± 1.6**	Russell *et al.* (1996a), this study
Semarkona (LL3.0) 4128-3-1	melilite	11–19	4.8–9.0	**5.4 ± 2.6**	This study
Quinyambie (LL3.4) 6076-5-1	melilite	3.6–52	1.1–20.7	**4.9 ± 1.3**	Russell *et al.* (1996a), this study
Moorabie (L3.8) 6302-2-1	hibonite	28–37	8.1–13.9	**5.2 ± 0.8**	This study
Dhajala (H3.8) DH-H1	hibonite	max ~17 200	max = 1064	**0.84 ± 0.05**	Hinton and Bischoff (1984), Ireland *et al.* (1992)
Clovis (H3.9) CAI	Plag (An_{84-96})	–	–	<0.18	Hutcheon *et al.* (1994)
Chondrules from UOCs					
Semarkona (LL3.0) CH4*	Glass	42–213	Up to 13.8	**0.87 ± 0.15**	Kita *et al.* (2000)
Semarkona (LL3.0) CH36*	Glass	45–289	Up to 12.1	**0.65 ± 0.18**	Kita *et al.* (2000)
Semarkona (LL3.0) CH60	Plag (~An_{70})	104–186	4.1–5.7	**0.47 ± 0.20**	Kita *et al.* (2000)
Semarkona (LL3.0) CH3	Plag (~An_{100})	76–108	2.5–6.0	**0.63 ± 0.22**	Kita *et al.* (2000)
Semarkona (LL3.0) CH23	Plag (~An_{100})	52	2.5	**0.69 ± 0.37**	Kita *et al.* (2000)
Semarkona (LL3.0) 1805-C5*	Glass	90	6.0	**0.96 ± 0.35**	McKeegan *et al.* (2000)
Bishunpur (LL3.1) CH4	Plag (~An_{90})	–	–	**1.0 ± 0.5**	Mostefaoui *et al.* (1999)
Bishunpur (LL3.1) CH18	Plag (~An_{91})	–	–	**0.56 ± 0.53**	Mostefaoui *et al.* (1999)
Bishunpur (LL3.1) 2359-C5*	Glass	43	2.5	**0.86 ± 0.56**	McKeegan *et al.* (2000)
Bishunpur (LL3.1) 2359-C8*	Glass	55–72	~3	**0.71 ± 0.40**	McKeegan *et al.* (2000)
Bishunpur (LL3.1) seven FeMg chondrules	Glass	20–170	–	**0.3 to 2.3**	Mostefaoui *et al.* (2000)
Inman (LL3.3) 5652-1-1	Plag (An_{95-98})	12–77	1.7–8.7	**1.1 ± 0.7**	Russell *et al.* (1996a), this study
Chainpur (LL3.4) 1251-3-1	Na-rich glass	50–60	2.7	**0.92 ± 0.24**	Russell *et al.* (1996a), this study
Semarkona (LL3.0) 4128-3-2	Plag (An_{84-93})	Up to 30	–	<1.7	This study
Semarkona (LL3.0) 4128-C8*	Glass	41	–	<1.0	McKeegan *et al.* (2000)
Semarkona (LL3.0) 4128-C5*	Glass	62	–	<0.8	McKeegan *et al.* (2000)
Krymka (LL3.1) 1729-9-1	Plag (An_{83-95})	Up to 92	–	<0.9	Russell *et al.* (1996a), this study
Chainpur (LL3.4) 1251-14-1	Plag (An_{82-90})	Up to 175	–	<0.2	Russell *et al.* (1996a), this study
Chainpur (LL3.4) 1251-14-2	Plag (An_{90-97})	Up to 410	–	<0.02	Russell *et al.* (1996a), this study
Chainpur (LL3.4) 1251-16-2	Plag (An_{78-85})	Up to 125	–	<0.4	This study
Chainpur (LL3.4) 1251-16-3	Na-rich glass	Up to 266	–	<0.12	This study
Chainpur (LL3.4) 5674-3b	Na-rich glass	Up to 510	–	<0.14	This study
Chainpur (LL3.4) 5674-2-1	Plag (An_{78-97})	Up to 300	–	<0.4	Russell *et al.* (1996a), this study
Quinyambie (LL3.4) 6076-5-2	Plag (An_{80-83})	Up to 85	–	<0.7	Russell *et al.* (1996a), this study
Manych (LL3.5) PC1	Plag (An_{80})	–	–	<0.04	Hutcheon and Jones (1995)
Manych (LL3.5) PC2	Plag (An_{75-85})	–	–	<0.03	Hutcheon and Jones (1995)
Ragland (LL3.5) chondrule	Plag (An_{77-80})	–	–	<1.0	Hutcheon *et al.* (1994)
Ikhrarene (L4) chondrule	Plag ($An_{??}$)	–	–	<0.13	Hutcheon *et al.* (1994)
Bovedy (L3.7) 1971,1	Plag (An_{77})	–	–	<0.012	Hutcheon *et al.* (1994)
Chondrules from C chondrites					
Acfer 094 (Canom) 094-1, 094-2	Plag ($An_{??}$)	402–69	2.0–6.2	**~1.2**	Hutcheon *et al.* (2000)
Efremovka (CV3) Al-rich chondrule	Plag ($An_{??}$)	72–80	2–3	**0.56 ± 0.33**	Hutcheon *et al.* (2000)
Efremovka (CV3) plag-rich chondrule	Plag ($An_{??}$)	–	–	**~1.0**	Marhas *et al.* (2000)
Efremovka (CV3) plag-rich chondrule	Plag ($An_{??}$)	40	–	**2.5 ± 0.8**	Srinivasan *et al.* (2000b)
Allende (CV3) POI 3510	Plag (An_{94})	75–130	2.0–7.0	**0.61**	Sheng *et al.* (1991)
Allende (CV3) POI 5ALLB6	Plag (An_{97})	130–222	1.2–6.0	**0.26**	Sheng *et al.* (1991)
Allende (CV3) plag-rich chondrule	Plag ($An_{??}$)	–	–	**~0.3**	Marhas *et al.* (2000)

TABLE 2. *Continued.*

Sample	High-Al Phase	$^{27}Al/^{24}Mg$	$\delta^{26}Mg$ (‰)	$(^{26}Al/^{27}Al)_0 \times 10^{-5}$†	Reference
Chondrules from C chondrites *(continued)*					
Axtell (CV3) AXCH1471	Plag (An_{95-97})	100–165	–	**0.34 ± 0.15**	Srinivasan *et al.* (2000a)
Axtell (CV3) three plag-rich chondrules	Plag (An_{90-98})	Up to 225	–	<0.3	Srinivasan *et al.* (2000a)
Allende (CV3) 10 POIs	–	–	–	<0.1	Sheng *et al.* (1991)
Coolidge (CV4) Cool 2-1, 2-2, 4-1	Plag (An_{95-99})	Up to 3000	–	<0.12 to <1.0	Russell *et al.* (1996b)
Kainsaz (CO3.2) KB1, KB2	Plag (An_{80})	–	–	<0.016	Hutcheon and Jones (1995)
Kainsaz (CO3.2) four Al-rich chondrules	Plag (An_{80})	–	–	<0.1 to <0.3	Hutcheon *et al.* (2000)
~18 chondrules from C chondrites	–	–	–	<0.1 to <1	Marhas *et al.* (2000)
Other materials from UOCs					
Semarkona (LL3.0) norite clast	Plag (An_{100})	–	–	**0.77 ± 0.21**	Hutcheon and Hutchison (1989)
Bovedy (L3.7) 1972 GB-1 glass	Glass	~12 000	21 ± 10	**0.03 ± 0.01**	Hutcheon *et al.* (1989)
St Marguerite (H4) plag grains	–	~5500	–	**0.02 ± 0.01**	Zinner and Göpel (1992)
Los Martinez (L6) plag clast	Plag (An_{18-55})	–	–	<1.1	Hutcheon *et al.* (1994)
Barwell (L6) basaltic clast	Plag (An_{42-74})	–	–	<0.0055	Hutcheon *et al.* (1994)
Tieschitz (H3.6) 1975 N1 clast	Plag (An_{68-83})	~123	–	<0.15	Hutcheon *et al.* (1989)
Parnallee (LL3.6) microgabbro	Plag (An_{70-75})	–	–	<0.4	Kennedy *et al.* (1992)

*Ferromagnesian chondrule.
†Clearly resolved initial ratios are given in bold type.

of several hundred thousand years for the CAI. This internal chronology for an individual CAI requires only that the object formed from a single material reservoir.

The above discussion ignores the rare isotopically distinctive inclusions (*e.g.*, FUN inclusions and hibonite-pyroxene spherules) whose low $(^{26}Al/^{27}Al)_0$ ratios cannot easily be explained in terms of chronology unless there is a mechanism for producing CAIs at a late stage while preserving large nuclear anomalies. The simple existence of these objects drives discussions of nebular heterogeneity, but the fact is that they are rare and appear to be exceptions to the general rule.

Aluminum-26 in Chondrules

Although chondrules are much more abundant in chondrites than CAIs (15–75% of the meteorite, depending on class; Grossman *et al.*, 1988), far fewer chondrules than CAIs have been analyzed for aluminum-magnesium systematics. Only recently have sufficient isotopic data from UOC chondrules with high Al/Mg ratios become available to make CAI-chondrule comparisons meaningful (this study; Kita *et al.*, 2000; Srinivasan *et al.*, 2000a,b; Hutcheon *et al.*, 2000; McKeegan *et al.*, 2000; Marhas *et al.*, 2000; Mostefaoui *et al.*, 2000). No good data yet exist for E-chondrite chondrules. The available data are summarized in Table 2 and Fig. 8. As with the data for CAIs, the chondrule data require careful evaluation to distinguish primary characteristics from those resulting from secondary processes.

The vast majority of UOC chondrules that show evidence of ^{26}Al come from Semarkona (LL3.0) and Bishunpur (LL3.1) (Table 2; Fig. 8). In these meteorites, most of the measured Al-chondrules and ferromagnesian chondrules have clear excesses of $^{26}Mg^*$. Inferred $(^{26}Al/^{27}Al)_0$ values for these chondrules range from 0.3×10^{-5} to 2.3×10^{-5} (Table 2). Chondrules from the same meteorites that do not show clear evidence of $^{26}Mg^*$ give upper limits on $(^{26}Al/^{27}Al)_0$ consistent with the same values (Fig. 8). Also, an olivine-pyroxene-anorthite clast from Semarkona, which has no obvious relationship with chondrules, exhibits $(^{26}Al/^{27}Al)_0 \approx (0.8 \pm 0.2) \times 10^{-5}$ (Hutcheon and Hutchison, 1989). The only chondrules measured to date that show good correlations between ^{26}Mg excesses and $^{27}Al/^{24}Mg$ (*i.e.*, undisturbed isochrons) are from Semarkona (Kita *et al.*, 2000), which is the least equilibrated ordinary chondrite known. Such correlations are the most convincing evidence that *in situ* decay of ^{26}Al was the actual source of ^{26}Mg excesses. The spread in initial ratios for chondrules appears to be relatively large, with ratios extending over nearly an order of magnitude (Fig. 8). It is unclear at present whether this spread is real, because the highest and lowest values are reported without uncertainties in a single abstract (Mostefaoui *et al.*, 2000). The error-weighted mean of the initial ratios for all type 3.0–3.1 UOC chondrules is 0.74×10^{-5}. In all but one case, the individual measurements are within the measurement uncertainty of the

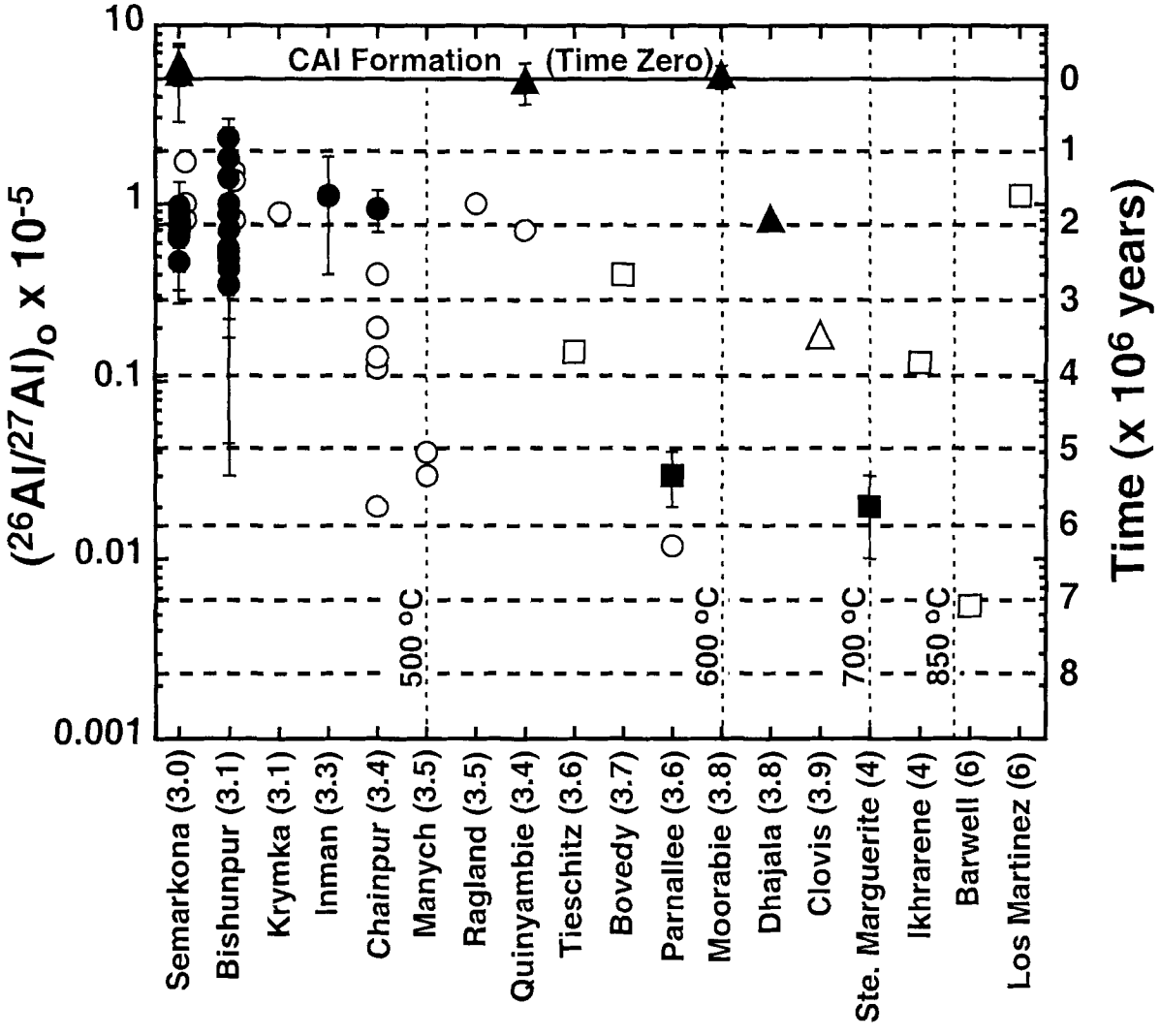

FIG. 8. All published $(^{26}Al/^{27}Al)_0$ ratios for CAIs (triangles), Al-chondrules and ferromagnesian chondrules (circles), and other Al-rich materials (squares) from UOCs are plotted as a function of the host meteorite's petrologic type. Filled symbols are clear detections of ^{26}Al, open symbols give upper limits on $(^{26}Al/^{27}Al)_0$. Dashed horizontal lines represent one-million-year time increments starting at CAI formation ($(^{26}Al/^{27}Al)_0 = 5 \times 10^{-5}$), assuming that all objects formed from the same homogeneous isotopic reservoir. Vertical dotted lines give approximate metamorphic temperatures for the host meteorites (this scale is not linear). Notice that for meteorites that have experienced <500 °C during metamorphism, there appears to be a clear upper limit on $(^{26}Al/^{27}Al)_0$ corresponding to a 1 to 2 Ma gap between the time when most CAIs formed and the time when chondrule formation began. The times indicated for non-CAIs with clear evidence for ^{26}Al from meteorites that have experienced ≥600 °C may reflect the end of parent-body metamorphism. Temperature estimates are based on Sears *et al.* (1991a), Huss and Lewis (1994), and Dodd (1981).

average value. Plagioclase from Al-chondrules and glass from ferromagnesian chondrules exhibit the same range of values for $(^{26}Al/^{27}Al)_0$. This similarity means that one can no longer argue (*e.g.*, Wood, 1996a) that the isotopic compositions of Al-chondrules may be unrelated to those of ferromagnesian chondrules.

No chondrules from meteorites of petrologic type 3.5 and higher show evidence of $^{26}Mg^*$. Three of five examples show low upper limits on $(^{26}Al/^{27}Al)_0$ of $<4 \times 10^{-7}$ to $<1 \times 10^{-7}$ (Table 2, Fig. 8). The contrast between these low values for $(^{26}Al/^{27}Al)_0$ and the high values in types 3.0–3.1 chondrites strongly suggests that metamorphic resetting of the magnesium-aluminum isotopic system has taken place in meteorites of petrologic type 3.5 and above (also see Kita *et al.*, 2000). This is consistent with expectations based on the diffusion rate of magnesium in anorthite (LaTourrette and Wasserburg, 1998).

Chainpur (LL3.4) is the most metamorphosed UOC in which a chondrule with clear evidence of $^{26}Mg^*$ has been found. Only one of seven Al-chondrules studied, Chainpur 1251-3-1, exhibits $^{26}Mg^*$ (in its glass), and the inferred ratio, $(^{26}Al/^{27}Al)_0 \approx (0.9 \pm 0.2) \times 10^{-5}$, is indistinguishable from those in chondrules from type 3.0–3.1 chondrites. No evidence for $^{26}Mg^*$ was found in two other glassy Al-chondrules or in four plagioclase-bearing Al-chondrules, all of which gave low

upper limits on $(^{26}Al/^{27}Al)_0$ similar to those of chondrules from type ≥3.5 meteorites (Table 2, Fig. 8). The interpretation of these data is not straightforward. Chainpur's estimated peak metamorphic temperature of ~450 °C (Sears *et al.*, 1991a; Huss and Lewis, 1994) was insufficient to eradicate the $^{26}Mg^*$ signatures in the plagioclase-bearing Al-chondrules within a reasonable time period. Homogenization of 10–50 μm thick anorthite laths requires a few × 10^7 to a few × 10^8 years (LaTourrette and Wasserburg, 1998). Also, the $^{26}Mg^*$ in Chainpur 1251-3-1 was detected in sodium-rich glass, yet glass might be expected to homogenize more quickly than anorthite. The long homogenization time for anorthite and the absence of $^{26}Mg^*$ in Chainpur anorthite imply either that the Chainpur chondrules that lack ^{26}Mg excesses formed with $(^{26}Al/^{27}Al)_0$ much lower than 1 × 10^{-5} or else that they were thermally reset at high temperatures before their incorporation into the final Chainpur parent body. In either case, an extended time period prior to final accretion of the Chainpur parent body is required if the differences in $(^{26}Al/^{27}Al)_0$ were due to decay of ^{26}Al.

In contrast to Chainpur, the isotopic data for chondrules from Semarkona and Bishunpur (also LL chondrites) are highly coherent (Table 2; Fig. 8). This might mean that Chainpur sampled a fundamentally different population of chondrules than did Semarkona and Bishunpur, but we think it more likely that Chainpur is a breccia consisting of both metamorphosed and relatively unmetamorphosed material from the LL-chondrite parent body. Supporting this idea is a disparity among different metamorphic thermometers (indicators of petrologic subtype) for Chainpur (*e.g.*, type 3.6 from thermoluminescence (TL) sensitivity, type 3.4 from ^{36}Ar, type 3.2/3.5 from wt% C; see Sears *et al.*, 1991a). Although not classified as such by those authors, this disparity suggests to us the possibility that Chainpur is a breccia like many other UOCs (Sears *et al.*, 1991a). Indeed, a majority of all chondrites may well be fragmental breccias (*e.g.*, Scott *et al.*, 1985). The $^{26}Mg^*$-bearing and $^{26}Mg^*$-free chondrules in Chainpur may have experienced different thermal histories resulting from an extended and complex parent-body history prior to final assembly.

In C chondrites, only ~20% of the Al-chondrules measured to date (9 of 49) bear evidence of *in situ* decay of ^{26}Al (Table 2). Considering the least-metamorphosed meteorites, two chondrules from the anomalous C chondrite Acfer 094 and three from the reduced CV3 Efremovka exhibit $(^{26}Al/^{27}Al)_0$ values between 0.5 × 10^{-5} and 2.5 × 10^{-5}. These initial ratios are essentially identical to those for chondrules from type 3.0–3.1 UOCs. Acfer 094 has apparently not experienced significant metamorphism (*e.g.*, Newton *et al.*, 1995). Efremovka is classified as CV3.2 by TL sensitivity (Guimon *et al.*, 1995) and the reported abundances of presolar grains suggest it has been heated more than either Semarkona or Bishunpur (cf., Huss, 1997 and references therein). However, the aluminum-magnesium isotopic data imply that Efremovka has not been heated to the same degree as has Chainpur. Three Al-chondrules (POIs) from Allende and one from Axtell give $(^{26}Al/^{27}Al)_0$ values between 0.3 × 10^{-5} and 0.6 × 10^{-5}. Numerous other chondrules from these two meteorites show no evidence of ^{26}Al and have upper limits on the initial ratios of $<0.1 \times 10^{-5}$ to $<0.3 \times 10^{-5}$. Allende and Axtell are oxidized CV3 chondrites, and there is evidence from abundances of presolar grains that these meteorites (or at least their matrix materials) have experienced temperatures of 550–600 °C, perhaps 250 °C higher than the reduced CV3 chondrites like Efremovka (Huss and Lewis, 1994; Huss *et al.*, 2000). Thus there may have been moderate metamorphic resetting of the ^{26}Al clock in chondrules from Allende and Axtell.

The accumulated $(^{26}Al/^{27}Al)_0$ data discussed above indicate that Al-chondrules and ferromagnesian chondrules are isotopically indistinguishable from each other. Evidence for ^{26}Al has been found in most types of chondrules, including types I, II, and III ferromagnesian chondrules (*e.g.*, Kita *et al.*, 2000) and anorthite-rich, forsterite-rich, and glassy Al-chondrules (*e.g.*, Sheng *et al.*, 1991; Russell *et al.*, 1996a). These isotopic data imply that Al-chondrules are true chondrules and not an unusual variety of CAI or some CAI-chondrule hybrid. Al-chondrules in UOCs are also isotopically indistinguishable from their counterparts in C chondrites. This conformity of isotopic data suggests that chondrules of all types and from C and O chondrites formed from an isotopic reservoir that was approximately homogenous with respect to ^{26}Al. Because C and O chondrites comprise over 90% of the meteorites in the world's meteorite collections, the data imply that this aluminum reservoir extended at least across the chondrite-forming region of the nebula.

Aluminum-26 Differences in Calcium-Aluminum-Rich Inclusions and Chondrules: Chronology or Nebular Heterogeneity?

There has been a vigorous debate about the interpretation of aluminum-magnesium isotopic differences between CAIs and chondrules since those differences first became apparent (*e.g.*, Hutcheon *et al.*, 1994; Cameron, 1995; Wood, 1996a; Russell *et al.*, 1996a; Kita *et al.*, 2000). Early papers pointed out deficiencies in the database that had to be filled to resolve the debate and significant progress has been made in acquiring these data. To the extent that CAIs and chondrules show consistent patterns across chondrite classes, we can evaluate nebular heterogeneity. To the extent that CAIs show consistently higher values of $(^{26}Al/^{27}Al)_0$ than chondrules, we may be able to evaluate their relative formation times and subsequent history. In this section, we reevaluate both chronological and non-chronological interpretations of the ^{26}Al database. We also identify outstanding issues that remain to be resolved.

A chronological interpretation of the aluminum-magnesium data assumes that the objects under investigation formed from a reservoir with a single initial $^{26}Al/^{27}Al$ ratio. In this case,

differences in $(^{26}Al/^{27}Al)_0$ can be ascribed solely to decay of ^{26}Al and thus interpreted in terms of formation time or time of later reprocessing. The strongest evidence that has been used to support this assumption is the observation that the majority of CAIs from diverse chondrite classes formed with $(^{26}Al/^{27}Al)_0$ of 4×10^{-5} to 5×10^{-5} (also see MacPherson *et al.*, 1995). Different chondrite classes are thought to represent accretion in different parts of the solar nebula. In turn, the CAI populations within each different chondrite type differ in size and, to some degree, in type. Accordingly some authors (*e.g.*, Russell *et al.*, 1998) suggest that the CAIs in each class originated in the nebular regions where they ultimately accreted. If so, then the Al-isotope reservoir from which all CAIs formed covered the chondrite-forming region and was, to first order, homogeneous in $^{26}Al/^{27}Al$. A similar argument can be made for Al-chondrules and ferromagnesian chondrules from both C and O chondrites, which formed with $(^{26}Al/^{27}Al)_0$ of $\sim 0.5 \times 10^{-5}$ to $\sim 2 \times 10^{-5}$ (Table 8). Assuming that chondrules also originated in the different regions where their host parent bodies finally accreted (*e.g.*, Wood, 1985), then the initial ratios in chondrules again imply that they came from a widespread, relatively homogeneous Al-isotope reservoir. Finally, if the CAIs and chondrules formed from the same reservoir, then the observed systematic difference in $(^{26}Al/^{27}Al)_0$ between CAIs and chondrules can be interpreted in terms of different formation times with the formation of most CAIs and the onset of chondrule formation being separated by about 2 Ma.

The chief evidence against homogeneous distribution of ^{26}Al is the existence of FUN inclusions. These objects contained very little ^{26}Al when they formed. They either formed (a) later than other CAIs, after ^{26}Al had decayed; (b) contemporaneously with other inclusions, but from isotopically different starting material (whether grains or a larger reservoir); (c) very early, before ^{26}Al was mixed into the solar system (*e.g.*, Sahijpal and Goswami, 1998); or (d) prior to the solar system and are in fact presolar grains (*e.g.*, Wood, 1998). Late formation of FUN inclusions requires that their relatively large isotopic anomalies in many elements can be preserved in spite of processes in the accretion disk that act to homogenize nebular material over time. The other possibilities explicitly require nebular heterogeneity of ^{26}Al at some scale. Although FUN inclusions remain unexplained, they are rare and may result from a special process. Recent data for ^{10}Be (MacPherson and Huss, 2001) hints that FUN inclusions may have formed in a different place than other CAIs, but where and from what remains unknown. Somewhat less compelling evidence against homogeneous distribution of ^{26}Al is the fact that the respective populations of unaltered CAIs and chondrules each appear to show significant spreads in their initial ratios. Some of the spread undoubtedly reflects analytical uncertainties, but some is probably real. Real spreads in the initial ratios could result from second-order heterogeneities in the distribution of ^{26}Al in the early solar system or from differences in formation times among groups of chondrules and CAIs on the order of a few $\times 10^5$ years. However, heterogeneities of up to ~20% across the chondrite-forming region would not change the basic features of a chronological interpretation of differences in $(^{26}Al/^{27}Al)_0$ between CAIs and chondrules or the timescales inferred for nebular processes.

The thorniest difficulty for the homogeneous distribution model (and hence chronologic interpretation of the isotopic data) arises out of the inferred one- to two-million-year interval between onset of CAI formation and formation of chondrules. The basic problem generally is stated in terms of how to keep millimeter- to centimeter-sized CAIs around in the solar nebula for 2 Ma waiting for chondrules to form. Objects of such size, including chondrules, would be expected to drift into the Sun in times on the order of 10^5 years due to gas drag (Weidenschilling, 1977; Cameron, 1995). One way to keep CAIs in the meteorite-forming region for millions of years is for them to accrete into kilometer-sized bodies. These bodies would have to be disrupted later in order for the fragments (CAIs) to re-accrete with chondrules to form the final chondrite parent bodies. However, brecciated clasts of composite CAI material are unknown. Moreover, very delicate CAIs (*e.g.*, "fluffy" type A inclusions) are well known in chondrites and it is far from clear how they would survive such a disruption process. An alternative possibility is that the CAIs did drift toward the Sun but were recycled back to the meteorite-forming region. Turbulent mixing in the accretion disk (*e.g.*, Morfill, 1983; Cameron, 1995) and recycling through bi-polar outflows (*e.g.*, Shu *et al.*, 1996) have been suggested, but neither of these ideas has been developed convincingly. What is generally overlooked in discussions of the two-million-year CAI-chondrule time gap is that evolutionary histories of individual CAIs require the same long duration. The magnesium isotopic heterogeneities observed in complex CAIs correlate with petrographic features produced by reheating after initial CAI formation (Podosek *et al.*, 1991). Much of this history is most plausibly interpreted in terms of nebular processes (*e.g.*, MacPherson and Davis, 1993). One study that attributed the complex isotopic signature in an individual CAI to nebular heterogeneity (Efremovka inclusion E2; Fahey *et al.*, 1987) was subsequently refuted by more detailed studies (Goswami *et al.*, 1994). In short, the extended nebular histories of individual CAIs pose as much, if not more, of a problem for astrophysical models as does the CAI-chondrule time gap. Some workers have argued that CAIs and chondrules were formed in protoplanetary environments and thus do not directly reflect nebular events (*e.g.*, Hsu *et al.*, 2000).

The alternative to an isotopically-homogeneous-nebula model (with its consequent implication for a chronological interpretation of ^{26}Al) is that materials with different initial ratios (*e.g.*, FUN CAIs, "normal" CAIs, chondrules) formed from distinct isotopic reservoirs. Two methods have been proposed to generate these isotopically distinct reservoirs: (1) the different isotopic reservoirs reflect incomplete mixing of material from different nucleosynthetic sources outside the

solar system, and (2) the ^{26}Al was produced locally within the early solar system.

Models that invoke incomplete mixing typically do not consider large-scale spatial heterogeneities in the nebula inherited from the presolar cloud (*e.g.*, Lee *et al.*, 1979), because such heterogeneities are difficult to maintain through the collapse of the molecular-cloud core and evolution of the accretion disk. However, there is no doubt that isotopic heterogeneities existed at some scale in the early solar system. Certainly, the individual presolar dust grains from which chondritic components ultimately formed were quite variable in their isotopic properties (*e.g.*, Zinner, 1997). The issue is whether the isotopic variations have the spatial scale and magnitude to map in an observable way onto chondrules and CAIs. As noted above, most models have been directed toward explaining the FUN inclusions. For example, Sahijpal and Goswami (1998) proposed that FUN CAIs formed prior to injection of ^{26}Al into the solar system. Wood (1998) proposed that FUN inclusions might have formed from aggregates of dust that originated in interstellar space before the astrophysical event that added ^{26}Al to the solar system and were melted by gas drag as they fell into the solar nebula. Both models rely on special circumstances for the formation of FUN inclusions and thus cannot be easily generalized. Wood (1996b) proposed an interesting model in which ^{26}Al was preferentially sited in a young, poorly crystallized fraction of the presolar dust, while older refractory grains preserved nuclear anomalies in other elements. Thermal processing in the solar system could have fractionated ^{26}Al-bearing material from ^{26}Al-poor refractory material, with FUN inclusions forming from the residual refractory dust and "normal" CAIs from more average nebula material. The main problem with generalizing this model is that it is difficult to devise a scenario that would give most CAIs one consistent $(^{26}Al/^{27}Al)_0$ ratio and chondrules a different ratio, rather than having a spread in $(^{26}Al/^{27}Al)_0$ among both chondrules and CAIs. It may well be a mistake to focus so much attention of FUN inclusions, which are rare and may have come from an unusual source or process. For example, the Wood (1996b) model might explain the FUN inclusions, while the difference in initial ratio between normal CAIs and chondrules reflects formation time. How and where FUN inclusions formed is not solved.

A more interesting class of heterogeneous-nebula models involves local production of ^{26}Al through local irradiation of solar system materials (*e.g.*, Heymann and Dziczkaniec, 1976; Clayton and Jin, 1995; Lee *et al.*, 1998). The biggest difficulty faced by these models is the fact that irradiation of average solar system matter by cosmic rays of typical energy and composition sufficient to produce CAI-levels of $(^{26}Al/^{27}Al)_0$ also produces other nuclides besides ^{26}Al (*e.g.*, Clayton *et al.*, 1977), but not in their proper relative abundances to ^{26}Al. To overcome this difficulty, modelers have proposed irradiation of a limited region of the nebula, irradiation of chemically fractionated material, and/or irradiation with cosmic rays of restricted energy distribution and composition (*e.g.*, Clayton and Jin, 1995; Lee *et al.*, 1998; Gounelle *et al.*, 2001). The most recent local-production models couple irradiation near the Sun to produce ^{26}Al with an X-wind model (*e.g.*, Shu *et al.*, 1996) to transport CAIs and other ^{26}Al-bearing objects out to the meteorite parent-body accretion regions (*e.g.*, Lee *et al.*, 1998; McKeegan *et al.*, 1998). This model builds on observations that young pre-main-sequence stars have powerful bipolar jets that could transfer material from near the central star out into the accretion disk, and it is driven by the desire to explain the Al-isotope differences between CAIs and chondrules. Local production of ^{26}Al provides an independent reservoir out of which the CAIs can form, and does so in an energetic physical environment conducive to CAI formation. The X-wind potentially provides a physical mechanism to keep the CAIs from falling onto the Sun before the chondrules form, and this is independent of whether ^{26}Al is locally produced or not. This last point is key: the local production component of the model suffers from a serious weakness that does not affect the X-wind element, namely producing ^{10}Be, ^{41}Ca, ^{53}Mn, and ^{26}Al in their proper relative abundances. Although there has been some recent success in constructing an irradiation model that can explain observed relative abundances of the short-lived radionuclides in CAIs (*e.g.*, Gounelle *et al.*, 2001), the conditions required for producing these radionuclides can only be satisfied with anomalous ^{3}He-rich, low-energy cosmic rays interacting with a specific core-mantle structure for the CAI precursors (Gounelle *et al.*, 2001). A cosmic-ray flux of protons and alpha particles with a more typical energy distribution and a plausible flux could have produced the observed abundances of ^{10}Be, ^{41}Ca, and ^{53}Mn in CAIs, but would have produced only a few percent of the necessary ^{26}Al (*e.g.*, Lee *et al.*, 1998; McKeegan *et al.*, 2000; Goswami *et al.*, 2001). In this case, most of the ^{26}Al would have been inherited from the presolar cloud.

The observation that CAIs from many chondrite classes have similar ^{16}O systematics is often cited as independent support for the idea that all CAIs formed in a single restricted location (*e.g.*, McKeegan *et al.*, 1998). But this does not require the production of ^{26}Al or even ^{16}O to be similarly restricted in space. Particle irradiation cannot explain the ^{16}O excesses that accompany ^{26}Al in CAIs (*e.g.*, Clayton *et al.*, 1977), although photodissociation of asymmetric molecules conceivably can (*e.g.*, Thiemens and Heidenreich, 1983). But even the latter case does not require a correlation between ^{16}O excesses and ^{26}Al because the effects in oxygen and aluminum are produced by fundamentally different mechanisms. Thus, although the oxygen isotopic data for CAIs may support the Shu *et al.* (1996) model for production of the CAIs in a near-Sun environment, it is not clear that those same data provide any constraints on the production (and hence distribution) of ^{26}Al or any other short-lived radionuclides.

In summary, the observations that most CAIs from a variety of chondrite classes formed with $(^{26}Al/^{27}Al)_0$ of $\sim 5 \times 10^{-5}$

and that chondrules from different classes formed with $(^{26}Al/^{27}Al)_0$ of ~1×10^{-5} are most consistent with a widespread and initially approximately uniform distribution of ^{26}Al in the nebula. Even though recent oxygen isotopic evidence hints at the possibility that CAIs themselves formed in a single restricted portion of the nebula, there is no mechanism that easily accounts for the ^{26}Al being similarly restricted. Together these arguments appear to make a reasonable case that differences in $(^{26}Al/^{27}Al)_0$ in different kinds of chondritic material can be interpreted, at least to first order, in terms of time.

The Timing of Events in the Early Solar System as Deduced from Aluminum-26

Given all of the new data now available and the arguments put forward above, it is instructive to examine the chronologic consequences of assuming that all objects did form from a single material reservoir that was homogeneous in $^{26}Al/^{27}Al$. Note that variations in $(^{26}Al/^{27}Al)_0$ on the order of 10–20% do not significantly affect these conclusions.

The macroscopic objects with the highest initial ratios are the CAIs; most formed with $(^{26}Al/^{27}Al)_0 = 4 \times 10^5$ to 5×10^5. Some of this spread undoubtedly reflects analytical uncertainty, but, interpreted strictly in terms of time, the spread implies a duration of ~2×10^5 years for CAI formation. The extended melting/re-melting chronologies of individual CAIs range from ~4×10^5 years (*e.g.*, for Allende CAI 5421; Hsu *et al.*, 2000) to more than 2 Ma for CAIs in which remelting followed secondary alteration that took place after most ^{26}Al decayed (MacPherson and Davis, 1993). In the latter case the melting—and hence the alteration that preceded it—is most plausibly interpreted as nebular and must have occurred prior to incorporation of the CAI into the meteorite in which it was found (*e.g.*, MacPherson and Davis, 1993), so the isotopic data constrain the time of final accretion of meteorite parent body to be at least 2 Ma later than the initial CAI formation.

Initial ratios of chondrules from unmetamorphosed chondrites are systematically lower than those of CAIs ($(^{26}Al/^{27}Al)_0 = 0.3 \times 10^{-5}$ to 2.3×10^{-5}). Again, some of the spread reflects analytical uncertainty, but taken at face value the spread implies a delay of 1 to 2 Ma between the onset of CAI formation and the time when chondrules began to form. The spread in the Semarkona data (0.47×10^{-5} to 0.96×10^{-5}) implies a duration for chondrule formation of ~7.5×10^5 years. Chondrules in Chainpur show a large range of $(^{26}Al/^{27}Al)_0$ values that cannot be interpreted solely in terms of metamorphism of the Chainpur parent body. The range in initial values among Chainpur chondrules implies that some chondrules formed or were last altered at least 2 Ma after the first chondrules formed. Adding the delay in the onset of chondrule formation to the time period over which chondrules appear to have been formed or modified prior to final accretion, the data appear to require a minimum of 4 Ma between the formation of the first CAI and the final accretion of Chainpur. However, initial accretion of kilometer-sized planetesimals may have been quite rapid (*e.g.*, Wood, 1985). The inferred 2 to 4 Ma timescale for formation of CAIs and chondrules and their accretion into meteorite parent bodies is broadly consistent with the lifetime of the solar nebula as inferred from theoretical models and observations of young pre-main-sequence stars (*e.g.*, reviews by Podosek and Cassen, 1994; Cameron, 1995).

The aluminum-magnesium data permit some preliminary statements on the timing of parent-body metamorphism. Aluminum-26 is potentially a very powerful heat source. If ^{26}Al was present in the early solar system at the canonical $^{26}Al/^{27}Al$ ratio of 5×10^{-5}, planetesimals of ~10 km in diameter would be heated to temperatures sufficient to metamorphose chondritic material over much of their interiors if they accreted within 2 to 3 Ma of the formation of CAIs (*e.g.*, LaTourrette and Wasserburg, 1998). The heat pulse would decay away in ~10 Ma. If one accepts that the low $(^{26}Al/^{27}Al)_0$ values in chondrules from type >3.5 ordinary chondrites and CAIs from >3.8 ordinary chondrites reflect parent-body metamorphism, then the low upper limits on $(^{26}Al/^{27}Al)_0$ in these objects indicate that they experienced a high-temperature interval that occurred—or extended until—at least 5 Ma after CAIs formed. Clear evidence of $^{26}Mg^*$ is found in objects from two meteorites that should have been heated sufficiently to destroy that evidence. A glassy clast from Bovedy (L3.7) gave $(^{26}Al/^{27}Al)_0 \approx 3 \times 10^{-7}$, and separated plagioclase crystals from Ste. Marguerite (H4) gave $(^{26}Al/^{27}Al)_0 \approx 2 \times 10^{-7}$ (Zinner and Göpel, 1992). There are two possible explanations for these results. One is that the $^{26}Mg^*$-bearing objects were introduced after metamorphism by impact gardening, as we proposed for Chainpur. The other is that the $^{26}Mg^*$-bearing material experienced the metamorphic event, and that the $(^{26}Al/^{27}Al)_0$ values reflect times when temperatures cooled enough for magnesium diffusion to stop. If this interpretation is correct, then Bovedy and Ste. Marguerite had cooled to the blocking temperature for the aluminum-magnesium system by ~5.5 to 6 Ma after CAIs formed. The upper limit on $(^{26}Al/^{27}Al)_0$ of $<5.5 \times 10^{-8}$ for a basaltic clast from the L6 chondrite, Barwell (Hutcheon *et al.*, 1994), implies that Barwell did not cool down until at least 7 Ma after CAIs formed. These times are consistent with ^{26}Al as the heat source for metamorphism and are made more plausible by the discovery in the Piplia Kalan Eucrite of evidence for ^{26}Al with a $(^{26}Al/^{27}Al)_0 \approx 1 \times 10^{-6}$, which implies a formation time for this brecciated basaltic meteorite of ~4 Ma years after CAIs (Srinivasan *et al.*, 1999, 2000c).

SUMMARY AND CONCLUSIONS

Clear evidence for the *in situ* decay of ^{26}Al has now been found in four UOC CAIs, with inferred $(^{26}Al/^{27}Al)_0$ ratios of ~5×10^{-5}. These data, along with oxygen-isotope data (McKeegan *et al.*, 1998; Russell *et al.*, 2000), show that the CAIs in UOCs are closely related to their counterparts in

carbonaceous chondrites. Only two of eleven Al-chondrules we measured from the same UOCs show clear evidence for ^{26}Al. The inferred $(^{26}Al/^{27}Al)_0$ ratios were $\sim 1 \times 10^{-5}$, clearly distinct from most CAIs and consistent with ratios observed in chondrules from type 3.0–3.1 UOCs and from lightly metamorphosed carbonaceous chondrites. The consistency of the isotopic systematics of carbonaceous and ordinary chondrites indicates that a chronological interpretation of the data is probably warranted. The timeline inferred from the ^{26}Al data suggests that CAIs formed over a few hundred thousand years, but experienced thermal reprocessing (including remelting) and secondary alteration for periods up to ~2 Ma. Chondrules began to form 1 to 2 Ma after the first CAIs. Accretion probably began relatively quickly after CAIs and chondrules formed, and the final meteorite parent bodies were apparently in place by 4 Ma after CAIs. Rapid accretion in the presence of ^{26}Al at the abundances indicated in CAIs and chondrules would mean that ^{26}Al was a potent heat source. Limited ^{26}Al data from metamorphosed meteorites indicates that metamorphism was over in type 4 chondrite parent bodies by 5 to 6 Ma after CAIs formed and continued in type 6 chondrites until after 7 Ma after CAIs formed. These times are consistent with ^{26}Al as a heat source. Isotopic heterogeneity does not appear to be responsible for most of the variations in $(^{26}Al/^{27}Al)_0$ observed among chondritic components, but FUN inclusions and other rare CAIs require a special explanation. Irradiation within the solar system, while capable of producing observed amounts of ^{10}Be, ^{41}Ca, and ^{53}Mn using reasonable fluxes and cosmic ray compositions, does not seem to be capable of simultaneously producing the inferred abundance of ^{26}Al.

Acknowledgements–This work was supported by NASA grants NAG5-4083 (G. J. W.), NAG5-8158 (G. R. H.), and NAG5-7396 (G. J. M.). Comments by two anonymous reviews and associate editor E. Zinner resulted in significant improvement to the paper and are gratefully acknowledged. Caltech Division Contribution #8651 (1043).

Editorial handling: E. Zinner

REFERENCES

BISCHOFF A. AND KEIL K. (1983) *Catalog of Al-rich Chondrules, Inclusions and Fragments in Ordinary Chondrites*. Spec. Publ. No. 22, Univ. of New Mexico, Institute of Meteoritics, Albuquerque, New Mexico, USA. 33 pp.

BISCHOFF A. AND KEIL K. (1984) Al-rich objects in ordinary chondrites: Related origin of carbonaceous and ordinary chondrites and their constitutents. *Geochim. Cosmochim. Acta* **48**, 693–709.

BRIGHAM C. A., HUTCHEON I. D., PAPANASTASSIOU D. A. AND WASSERBURG G. J. (1986) Evidence for ^{26}Al and Mg isotopic heterogeneity in a fine-grained CAI (abstract). *Lunar Planet. Sci.* **17**, 85–86.

CAMERON A. G. W. (1995) The first ten million years in the solar nebula. *Meteoritics* **30**, 133–161.

CATANZARO E. J., MURPHY T. J., GARNER E. L. AND SHIELDS W. R. (1966) Absolute isotopic abundance ratios and atomic weights of magnesium. *J. Res NBS* **70A**, 453–458.

CLAYTON D. D. AND JIN L. (1995) A new interpretation of ^{26}Al in meteoritic inclusions. *Astrophys. J.* **451**, L87–L91.

CLAYTON D. D., DWEK E. AND WOOSLEY S. E. (1977) Isotopic anomalies and proton irradiation in the early solar system. *Astrophys. J.* **214**, 300–315.

DODD R. T. (1981) *Meteorites*. Cambridge University Press, Cambridge, U.K. 368 pp.

FAGAN T. J., KROT A. N. AND KEIL K. (2000) Calcium-aluminum-rich inclusions in enstatite chondrites (I): Mineralogy and textures. *Meteorit. Planet. Sci.* **35**, 771–781.

FAGAN T. J., MCKEEGAN K. D., KROT A. N. AND KEIL K. (2001) Calcium-aluminum-rich inclusions in enstatite chondrites (II): Oxygen isotopes. *Meteorit. Planet. Sci.* **36**, 223–230.

FAHEY A. J., ZINNER E. K., CROZAZ G. AND KORNACKI A. S. (1987) Microdistributions of Mg isotopes and REE abundances in a Type A calcium-aluminium-rich inclusion from Efremovka. *Geochim. Cosmochim. Acta* **51**, 3215–3229.

GOSWAMI J. N., SRINIVASAN G. AND ULYANOV A. A. (1994) Ion microprobe studies of Efremovka CAIs: I. Magnesium isotope composition. *Geochim. Cosmochim. Acta* **58**, 431–447.

GOSWAMI J. N., MARHAS K. K. AND SAHIJPAL S. (2001) Did solar energetic particles produce the short-lived nuclides present in the early solar system? *Astrophys. J.* **549**, 1151–1159.

GOUNELLE M., SHU F. H., SHANG H., GLASSGOLD A. E., REHN K. E. AND LEE T. (2001) Extinct radioactivities and protosolar cosmic-rays: Shelf-shielding and light elements. *Astrophys. J.* **548**, 1051–1070.

GROSSMAN J. N., RUBIN A. E., NAGAHARA H. AND KING E. A. (1988) Properties of chondrules. In *Meteorites and the Early Solar System* (eds. J. F. Kerridge and M. S. Mathews), pp. 619–659. Univ. Arizona Press, Tucson, Arizona, USA.

GUAN Y., HUSS G. R., MACPHERSON G. J. AND WASSERBURG G. J. (2000a) Calcium-aluminum-rich inclusions from enstatite chondrites: Indigenous or foreign? *Science* **289**, 1330–1333.

GUAN Y., MCKEEGAN K. D. AND MACPHERSON G. J. (2000b) Oxygen-isotopic compositions in two calcium-aluminum-rich inclusions from unequilibrated ordinary chondrites (abstract). *Meteorit. Planet. Sci.* **35 (Suppl.)**, A67.

GUAN Y., MCKEEGAN K. D. AND MACPHERSON G. J. (2000c) Oxygen isotopes in calcium-aluminum-rich inclusions from enstatite chondrites: New evidence for a single CAI source in the solar nebula. *Earth Planet. Sci. Lett.* **181**, 271–277.

GUIMON R. K., SYMES S. K. J., SEARS D. W. G. AND BENOIT P. H. (1995) Chemical and physical studies of type 3 chondrites XII: The metamorphic history of CV chondrites and their components. *Meteoritics* **30**, 704–714.

HEYMANN D. AND DZICZKANIEC M. (1976) Early irradiation of matter in the solar system: Magnesium (proton, neutron) scheme. *Science* **191**, 79–81.

HINTON R. W. AND BISCHOFF A. (1984) Ion microprobe magnesium isotope analysis of plagioclase and hibonite from ordinary chondrites. *Nature* **308**, 169–172.

HUNEKE J. C., ARMSTRONG J. T. AND WASSERBURG G. J. (1983) FUN with PANURGE: High mass resolution ion microprobe measurements of Mg in Allende inclusions. *Geochim. Cosmochim. Acta* **47**, 1635–1650.

HSU W., WASSERBURG G. J. AND HUSS G. R. (2000) High time resolution by use of the ^{26}Al chronometer in the multistage formation of a CAI. *Earth Planet. Sci. Lett.* **182**, 15–29.

HUSS G. R. (1997) The survival of presolar grains in solar system bodies. In *Astrophysical Implications of the Laboratory Study of Presolar Materials* (eds. T. J. Bernatowicz and E. K. Zinner), pp. 721–748. AIP Press, Woodbury, New York, USA.

HUSS G. R. AND LEWIS R. S. (1994) Noble gases in presolar diamonds II: Component abundances reflect thermal processing. *Meteoritics* **29**, 811–829.

HUSS G. R., MESHIK A. P. AND HOHENBERG C. M. (2000) Abundances of presolar grains in Renazzo and Axtell: Implications for their thermal histories (abstract). *Lunar Planet. Sci.* **31**, #1467, Lunar and Planetary Institute, Houston, Texas, USA (CD-ROM).

HUTCHEON I. D. AND HUTCHISON R. (1989) Evidence from the Semarkona ordinary chondrite for ^{26}Al heating of small planets. *Nature* **337**, 238–241.

HUTCHEON I. D. AND JONES R. H. (1995) The ^{26}Al-^{26}Mg record of chondrules: Clues to nebular chronology (abstract). *Lunar Planet. Sci.* **26**, 647–648.

HUTCHEON I. D. AND NEWTON R. C. (1981) Mg isotopes, mineralogy, and mode of formation of secondary phases in C3 refractory inclusions (abstract). *Lunar Planet. Sci.* **12**, 491–492.

HUTCHEON I. D., HUTCHISON R. AND KENNEDY A. (1989) Mg isotopes and rare earth abundances in plagioclase from ordinary chondrites: A search for ^{26}Al (abstract). *Lunar Planet. Sci.* **20**, 434–435.

HUTCHEON I. D., HUSS G. R. AND WASSERBURG G. J. (1994) A search for ^{26}Al in chondrites: Chondrule formation time scales (abstract). *Lunar Planet. Sci.* **25**, 587–588.

HUTCHEON I. D., KROT A. N. AND ULYANOV A. A. (2000) ^{26}Al in anorthite-rich chondrules in primitive carbonaceous chondrites: Evidence chondrules postdate CAI (abstract). *Lunar Planet. Sci.* **31**, #1869, Lunar and Planetary Institute, Houston, Texas, USA (CD-ROM).

IRELAND T. R., FAHEY A. J. AND ZINNER E. K. (1991) Hibonite-bearing microspherules: A new type of refractory inclusion with large isotopic anomalies. *Geochim. Cosmochim Acta* **55**, 367–379.

IRELAND T. R., ZINNER E. K., FAHEY A. J. AND ESAT T. M. (1992) Evidence for distillation in the formation of HAL and related hibonite inclusions. *Geochim. Cosmochim. Acta* **56**, 2503–2520.

KENNEDY A. K., HUTCHISON R., HUTCHEON I. D. AND AGRELL S. O. (1992) A unique high Mn/Fe microgabbro in the Parnallee (LL3) ordinary chondrite: Nebular mixture of planetary differentiate from a previously unrecognized planetary body? *Earth Planet. Sci. Lett.* **113**, 191–205.

KITA N. T., NAGAHARA H., TOGASHI S. AND MORISHITA Y. (2000) A short formation period of chondrules in the solar nebula. *Geochim. Cosmochim. Acta* **64**, 3913–3922.

LATOURRETTE T. AND WASSERBURG G. J. (1998) Mg diffusion in anorthite: Implications for the formation of early solar system planetesimals. *Earth Planet. Sci. Lett.* **158**, 91–108.

LEE T., PAPANASTASSIOU D. AND WASSERBURG G. J. (1976) Demonstration of ^{26}Mg excess in Allende and evidence of ^{26}Al. *Geophys. Res. Lett.* **3**, 109–112.

LEE T., PAPANASTASSIOU D. AND WASSERBURG G. J. (1977) Aluminum-26 in the early solar system: Fossil or fuel? *Astrophys. J.* **211**, L107–L110.

LEE T., RUSSELL W. A. AND WASSERBURG G. J. (1979) Calcium isotopic anomalies and the lack of aluminum-26 in an unusual Allende inclusion. *Astrophys. J.* **228**, L93–L98.

LEE T., SHU F. H., SHANG H., GLASSGOLD A. E. AND REHM K. E. (1998) Protostellar cosmic rays and extinct radioactivities in meteorites. *Astrophys. J.* **506**, 898–912.

MACPHERSON G. J. AND DAVIS A. M. (1993) A petrologic and ion microprobe study of a Vigarano Type B refractory inclusion. Evolution by multiple stages of alteration and melting. *Geochim. Cosmochim. Acta* **57**, 231–243.

MACPHERSON G. J. AND HUSS G. R. (2000) Convergent evolution of CAIs and chondrules: Evidence from bulk compositions and a cosmochemical phase diagram (abstract). *Lunar Planet. Sci.* **31**, #1796, Lunar and Planetary Institute, Houston, Texas, USA (CD-ROM).

MACPHERSON G. J. AND HUSS G. R. (2001) Extinct ^{10}Be in CAIs from Vigarano, Leoville, and Axtell (abstract). *Lunar Planet. Sci.* **32**, #1882, Lunar and Planetary Institute, Houston, Texas, USA (CD-ROM).

MACPHERSON G. J., WARK D. A. AND ARMSTRONG J. T. (1988) Primitive material surviving in chondrites: Refractory inclusions. In *Meteorites and the Early Solar System* (eds. J. F. Kerridge and M. S. Mathews), pp. 746–807. Univ. Arizona Press, Tucson, Arizona, USA.

MACPHERSON G. J., DAVIS A. M. AND ZINNER E. K. (1995) The distribution of ^{26}Al in the early solar system—A reappraisal. *Meteoritics* **30**, 365–386.

MARHAS K. K., HUTCHEON I. D., KROT A. N., GOSWAMI J. N. AND KOMATSU M. (2000) Aluminum-26 in carbonaceous chondrite chondrules (abstract). *Meteorit. Planet. Sci.* **35 (Suppl.)**, A102.

MCKEEGAN K. D., LESHIN L. A., RUSSELL S. S. AND MACPHERSON G. J. (1998) Oxygen isotopic abundances in calcium-aluminum-rich inclusions from ordinary chondrites: Implications for nebular heterogeneity. *Science* **280**, 414–418.

MCKEEGAN K. D., GREENWOOD J. P., LESHIN L. AND COSARINSKY M. (2000) Abundance of ^{26}Al in ferromagnesian chondrules of unequilibrated ordinary chondrites (abstract). *Lunar Planet. Sci.* **31**, #2009, Lunar and Planetary Institute, Houston, Texas, USA (CD-ROM).

MORFILL G. E. (1983) Some cosmochemical consequences of a turbulent protoplanetary cloud. *Icarus* **53**, 41–54.

MOSTEFAOUI S., KITA N. T., NAGAHARA H., TOGASHI S. AND MORISHITA Y. (1999) Aluminum-26 in two ferromagnesian chondrules from a highly unequilibrated ordinary chondrite: Evidence of a short period of chondrule formation (abstract). *Meteorit. Planet. Sci.* **34 (Suppl.)**, A84.

MOSTEFAOUI S., KITA N. T., TACHIBANA S., NAGAHARA H., TOGASHI S. AND MORISHITA Y. (2000) Correlated initial aluminum-26/aluminum-27 with olivine and pyroxene proportions in chondrules from highly unequilibrated ordinary chondrites (abstract). *Meteorit. Planet. Sci.* **35 (Suppl.)**, A114.

NEWTON J., BISCHOFF A., ARDEN J. W., FRANCHI I. A., GEIGER T., GRESHAKE A. AND PILLINGER C. T. (1995) Acfer 094, a uniquely primitive carbonaceous chondrite from the Sahara. *Meteoritics* **30**, 47–56.

PODOSEK F. A. AND CASSEN P. (1994) Theoretical, observational, and isotopic estimates of the lifetime of the solar nebula. *Meteoritics* **29**, 6–25.

PODOSEK F. A., ZINNER E. K., MACPHERSON G. J., LUNDBERG L. L., BRANNON J. C. AND FAHEY A. J. (1991) Correlated study of initial ^{87}Sr/^{86}Sr and Al-Mg isotopic systematics and petrologic properties in a suite of refractory inclusions from the Allende meteorite. *Geochim. Cosmochim. Acta* **55**, 1083–1110.

RUSSELL S. S., SRINIVASAN G., HUSS G. R., WASSERBURG G. J. AND MACPHERSON G. J. (1996a) Evidence for widespread ^{26}Al in the solar nebula and new constraints for nebula timescales. *Science* **273**, 757–762.

RUSSELL S. S., HUSS G. R., WASSERBURG G. J. AND MACPHERSON G. J. (1996b) Plagioclase-rich inclusions from the Coolidge meteorite: A distinct CAI population with no evidence for radiogenic ^{26}Mg (abstract). *Meteorit. Planet. Sci.* **31 (Suppl.)**, A119–A120.

RUSSELL S. S., HUSS G. R., MACPHERSON G. J. AND WASSERBURG G. J. (1997) Early and late chondrule formation: New constraints for solar nebula chronology from ^{26}Al/^{27}Al in unequilibrated ordinary chondrites (abstract). *Lunar Planet. Sci.* **28**, 1209–1210.

RUSSELL S. S., HUSS G. R., FAHEY A. J., GREENWOOD R. C., HUTCHISON R. AND WASSERBURG G. J. (1998) An isotopic and petrologic study of calcium-aluminum-rich inclusions from CO3 meteorites. *Geochim. Cosmochim. Acta* **62**, 689–714.

RUSSELL S. S., MACPHERSON G. J., LESHIN L. A. AND MCKEEGAN K. D. (2000) ^{16}O enrichments in aluminum-rich chondrules from ordinary chondrites. *Earth Planet. Sci. Lett.* **184**, 57–74.

SAHIJPAL S. AND GOSWAMI J. N. (1998) Refractory phases in primitive meteorites devoid of ^{26}Al and ^{41}Ca: Representative samples of first solar system solids? *Astrophys. J.* **509**, L137–L140.

SCOTT E. R. D., LUSBY D. AND KEIL K. (1985) Ubiquitous brecciation after metamorphism in equilibrated ordinary chondrites. *Proc. Lunar Planet. Sci. Conf.* **16th**, *J. Geophys. Res.* **90 Suppl.**, D137–D148.

SEARS D. W. G., HASAN F. A., BATCHELOR J. D. AND LU J. (1991a) Chemical and physical studies of type 3 chondrites–XI: Metamorphism, pairing, and brecciation of ordinary chondrites. *Proc. Lunar Planet. Sci. Conf.* **21st**, 493–512.

SEARS D. W. G., BATCHELOR J. D., LU. J. AND KECK B. D. (1991b) Metamorphism of CO and CO-like chondrites and comparisons with type 3 ordinary chondrites. *Proc. NIPR Symp. Antarct. Meteorites* **4**, 319–343.

SHENG Y. J., HUTCHEON I. D. AND WASSERBURG G. J. (1991) Origin of plagioclase-olivine inclusions in carbonaceous chondrites. *Geochim. Cosmochim. Acta* **55**, 581–599.

SHU F. H., SHANG H. AND LEE T. (1996) Toward an astrophysical theory of chondrites. *Science* **271**, 1545–1552.

SRINIVASAN G., RUSSELL S. S., MACPHERSON G. J., HUSS G. R. AND WASSERBURG G. J. (1996) New evidence for ^{26}Al in CAI and chondrules from type 3 ordinary chondrites (abstract). *Lunar Planet. Sci.* **27**, 1257–1258.

SRINIVASAN G., GOSWAMI J. N. AND BHANDARI N. (1999) Al-26 in eucrite Piplia Kalan: Plausible heat source and formation chronology. *Science* **284**, 1348–1350.

SRINIVASAN G., HUSS G. R. AND WASSERBURG G. J. (2000a) A petrographic, chemical and isotopic study of calcium-aluminum-rich inclusions and aluminum-rich chondrules from the Axtell (CV3) chondrite. *Meteorit. Planet. Sci.* **35**, 1333–1354.

SRINIVASAN G., KROT A. N. AND ULYANOV A. A. (2000b) Aluminum-magnesium systematics in anorthite-rich chondrules and calcium-aluminum-rich inclusions from the reduced CV chondrite Efremovka (abstract). *Meteorit. Planet. Sci.* **35 (Suppl.)**, A151–A152.

SRINIVASAN G., PAPANASTASSIOU D. A., WASSERBURG G. J., BHANDARI N. AND GOSWAMI J. N. (2000c) Re-examination of $^{26}Al/^{26}Mg$ systematics in the Piplia Kalan eucrite (abstract). *Lunar Planet. Sci.* **31**, #1795, Lunar and Planetary Institute, Houston, Texas, USA (CD-ROM).

THIEMENS M. H. AND HEIDENREICH J. E. (1983) The mass independent fractionation of oxygen: A novel isotope effect and its possible cosmochemical implications. *Science* **219**, 1073–1075.

WASSERBURG G. J. AND PAPANASTASSIOU D. A. (1982) Some short-lived isotopes in the early solar system-a connection with the placental ISM. In *Essays in Nuclear Astrophysics* (eds. C. A. Barnes, D. D. Clayton and D. N. Schramm), pp. 77–140. Cambridge Univ. Press, Cambridge, U.K.

WASSERBURG G. J., LEE T. AND PAPANASTASSIOU D. A. (1977) Correlated O and Mg isotopic anomalies in Allende inclusions: II. Magnesium. *Geophys. Res. Lett.* **4**, 299–302.

WEIDENSCHILLING S. J. (1977) Aerodynamics of solid bodies in the solar nebula. *Mon. Not. R. Astron. Soc.* **180**, 57–70.

WLOTZKA F. (1985) Olivine-spinel and olivine-ilmenite thermometry in chondrites of different petrologic type (abstract). *Lunar Planet. Sci.* **16**, 918–919.

WOOD J. A. (1985) Meteoritic constraints on processes in the solar nebula. In *Protostars and Planets II* (eds. D. C. Black and M. S. Mathews), pp. 687–702. Univ. Arizona Press, Tucson, Arizona, USA.

WOOD J. A. (1996a) Unresolved issues in the formation of chondrules and chondrites. In *Chondrules and the Protoplanetary Disk* (eds. R. H. Hewins, R. H. Jones and E. R. D. Scott), pp. 55–69. Cambridge Univ. Press, Cambridge, U.K.

WOOD J. A. (1996b) Why did some CAIs contain ^{26}Al and others not? (abstract). *Meteorit. Planet. Sci.* **31 (Suppl.)**, A154–A155.

WOOD J. A. (1998) Meteoritic evidence for the infall of large interstellar dust aggregates during the formation of the solar system. *Astrophys. J.* **503**, L101–L104.

ZINNER E. K. (1997) Presolar material in meteorites: An overview. In *Astrophysical Implications of the Laboratory Study of Presolar Materials* (eds. T. J. Bernatowicz and E. K. Zinner), pp. 3–26. AIP Press, Woodbury, New York, USA.

ZINNER E. K. AND GÖPEL C. (1992) Evidence for ^{26}Al in feldspars from the H4 chondrite Ste. Marguerite (abstract). *Meteoritics* **27**, 311–312.